AD_____

Award Number: W81XWH-07-1-0153

TITLE: Examination of the Role of DNA Methylation Changes in Prostate Cancer using the Transgenic Adenocarcinoma of Mouse Prostate (TRAMP) Model

PRINCIPAL INVESTIGATOR: Shannon R. Morey Kinney

CONTRACTING ORGANIZATION: Roswell Park Cancer Institute
Buffalo, NY 14263

REPORT DATE: March 2009

TYPE OF REPORT: Annual Summary

PREPARED FOR: U.S. Army Medical Research and Materiel Command
Fort Detrick, Maryland 21702-5012

REPORT DOCUMENTATION PAGE

Form Approved
OMB No. 0704-0188

1. REPORT DATE	2. REPORT TYPE	3. DATES COVERED
1 Mar 2009	Annual Summary	1 Mar 2008 – 28 Feb 2009

4. TITLE AND SUBTITLE

Examination of the Role of DNA Methylation Changes in Prostate Cancer using the Transgenic Adenocarcinoma of Mouse Prostate (TRAMP) Model

5a. CONTRACT NUMBER

5b. GRANT NUMBER
W81XWH-07-1-0153

5c. PROGRAM ELEMENT NUMBER

6. AUTHOR(S)

Shannon R. Morey Kinney

E-Mail: shannon.moreykinney@roswellpark.org

5d. PROJECT NUMBER

5e. TASK NUMBER

5f. WORK UNIT NUMBER

7. PERFORMING ORGANIZATION NAME(S) AND ADDRESS(ES)

Roswell Park Cancer Institute
Buffalo, NY 14263

8. PERFORMING ORGANIZATION REPORT NUMBER

9. SPONSORING / MONITORING AGENCY NAME(S) AND ADDRESS(ES)
U.S. Army Medical Research and Materiel Command
Fort Detrick, Maryland 21702-5012

10. SPONSOR/MONITOR'S ACRONYM(S)

11. SPONSOR/MONITOR'S REPORT NUMBER(S)

12. DISTRIBUTION / AVAILABILITY STATEMENT
Approved for Public Release; Distribution Unlimited

13. SUPPLEMENTARY NOTES

14. ABSTRACT
We have previously shown that Transgenic Adenocarcinoma of Mouse Prostate (TRAMP) tumors display altered DNA methyltransferase (Dnmt) expression and DNA methylation patterns, such that global DNA hypomethylation occurs early, while locus specific DNA hypermethylation occurs late during TRAMP tumor progression. In addition, we have identified several genes (Gsts, Mgmt, Pdlim4, and Zfp185), that are commonly silenced by promoter hypermethylation in human prostate cancer, that are also downregulated in TRAMP tumors. However, in TRAMP these genes do not display promoter hypermethylation. Although further studies suggest that other epigenetic mechanisms may be playing a role in the transcriptional regulation of these genes. Using a TRAMP Dnmt1 hypomorphic mouse model, we have tested the role of Dnmt1 in prostate cancer progression. At an early time point hypomorphic mice display advanced tumor progression and at a later time point hypomorphic mice have repressed tumor progression and metastases. These results suggest that both global hypomethylation and locus specific hypermethylation are important events during TRAMP tumorigenesis. This indicates a dual role for Dnmt1 in TRAMP tumor progression with a suppressive role in early stage disease and oncogenic role at later stages.

15. SUBJECT TERMS
Prostate cancer, DNA methylation, Transgenic Adenocarcinoma of Mouse Prostate (TRAMP)

16. SECURITY CLASSIFICATION OF:			17. LIMITATION OF ABSTRACT	18. NUMBER OF PAGES	19a. NAME OF RESPONSIBLE PERSON
a. REPORT	b. ABSTRACT	c. THIS PAGE			USAMRMC
U	U	U	UU		19b. TELEPHONE NUMBER *(include area code)*

Table of Contents

Introduction:

DNA hypermethylation of tumor suppressor gene promoters, in conjunction with hypomethylation of repetitive elements and increased expression of DNA methyltransferases (DNMTs), occurs in human prostate cancer. An understanding of how DNA methylation becomes deregulated in prostate cancer and how to reverse or prevent this process is important for developing anticancer therapies. It has also been shown that pharmacological inhibition of DNMTs can have anticancer effects, supporting the concept that hypomethylation and thus re-expression of tumor suppressor genes may have therapeutic significance in the treatment of cancer. The TRansgenic Adenocarcinoma of Mouse Prostate (TRAMP) SV40 transgenic model provides an excellent system to study disruption of the DNA methylation process in prostate cancer and to determine whether inhibition of DNMTs abrogates prostate tumorigenesis. We have shown that DNA methylation is deregulated in the TRAMP model, which is characterized by significantly increased DNMT activity and expression, repetitive element and global hypomethylation beginning at early stages, and locus specific hypermethylation predominantly in late stage disease. Based on these findings, we hypothesize that aberrant DNA methylation contributes to TRAMP tumorigenesis, and that disruption of DNMTs will inhibit prostate oncogenesis in TRAMP. The information gained from this study will permit a better understanding of the role of aberrant DNA methylation in prostate cancer.

Specific Aims:

1. Identify and characterize the biological significance of genes that have altered DNA methylation status in TRAMP.
2. Determine whether genetic disruption of DNMT1 inhibits prostate tumorigenesis in TRAMP.

Body:

Examination of the Role of DNA Methylation Changes in Prostate Cancer using the Transgenic Adenocarcinoma of Mouse Prostate (TRAMP) Model

Task 1. Identify and characterize the biological significance of genes that have altered DNA methylation status in TRAMP:

As outlined in my previous Summary Report, we were unable to identify promoter hypermethylation correlating with decreased gene expression, except in the case of Irx3, using Restriction Landmark Genomic Scanning (RLGS) analysis of several types of TRAMP tumors (1-3). At that time I mentioned several candidate tumor suppressor genes that are commonly hypermethylated in the promoter region associated with decreased expression, in human prostate cancer. These genes are Aldh1a2, Mgmt, Pdlim4, and Zfp185. mRNA expression was examined first in normal mouse prostate and compared that to several stages of TRAMP tumors. All of these genes, except Aldh1a2, displayed decreased mRNA expression in most of the eight tumors analyzed as compared to normal prostate (Fig 1a-d). This indicated that the transcription of these three genes (Mgmt, Pdlim4, and Zfp185) is being down regulated and DNA methylation is one possible mechanism for this. Based on these results, traditional bisulfite sequencing analysis was utilized to examine the methylation status of the promoters of these genes. Two normal mouse prostate samples and the two TRAMP tumor samples that displayed the most decrease in mRNA expression as compared to control for each gene were analyzed. However, the results showed that there was no hypermethylation of the region of the gene promoter that was analyzed in normal prostates with only very slight increases in TRAMP tumors (Fig. 2a-c). It remains possible that a region of the promoter we did not analyze is hypermethylated, resulting in the observed decreased expression of Mgmt, Pdlim4, and Zfp185. However, these results suggest that a different mechanism is utilized by the tumor cells to inhibit the expression of these genes.

The above described results are similar to findings of another study from our laboratory, wherein we examined the family of Glutathione S-Transferase (Gst) genes, which are also commonly hypermethylated in human prostate cancer (4). We examined mRNA expression in TRAMP tumors compared to normal prostate and found that mRNA and protein levels of the Gst genes are decreased as expected (4). However, similar to the results described above for Mgmt, Pdlim4, and Zfp185, there was no clear increase of DNA methylation in the promoters of the Gst genes in TRAMP tumors as compared to normal prostate (4). Further experiments did reveal that combined treatment of a TRAMP cell line with a hypomethylating agent and histone deacetylase inhibitor resulted in increased expression of Gst genes supporting the idea that histone modifications, a different epigenetic component, may be playing a role in the regulation of the Gst genes (4). This may also be true for the Mgmt, Pdlim4, and Zfp185, but promoter DNA methylation does not seem to be regulating the expression of these genes.

I previously proposed to utilize a microarray based technique in my alternative approaches in the case that RLGS or analysis of candidate genes was not sufficient to identify genes that display promoter hypermethylation in TRAMP tumors. At the time of my previous Summary Report, I was optimizing the protocol for methyl-DIP chip array analyses to compare TRAMP tumors to normal prostate and identify novel genes that fit these criteria. However, I had some technical difficulties with sample preparation for methyl-DIP analysis and since then we have begun a collaboration with Dr. John Greally at The Albert Einstein Institute to utilize a very similar but technically improved assay, HpaII Tiny Fragment Enrichment by Ligation-Mediated PCR (HELP). The array that is used for this assay is a Nimblegen tiling array, designed by Dr. Greally, which covers the entire mouse

genome. Currently, I have completed the sample preparation for both normal prostates and TRAMP tumors and sent them to Nimblegen for the arrays to be done. Once the arrays have been completed on a small set of samples, we will analyze the results and identify a subset of hypermethylated genes. We will then measure DNA methylation of these genes in a large set of samples by MassArray or Pyrosequencing techniques to both confirm the HELP results and determine if any of those genes are commonly hypermethylated in TRAMP. If genes are identified that are commonly hypermethylated in their promoter regions, further experiments may be done, such as qRT-PCR analyses to determine mRNA expression of those genes.

Task 2. Determine whether genetic disruption of DNA methyltransferase 1 (DNMT1) inhibits prostate tumorigenesis in TRAMP:

One goal of this task is to produce 50:50 C57Bl/6 x FVB DNMT1 hypomorphic TRAMP mice. I have established and maintain colonies of R/+ and N/+ mice that have been backcrossed to FVB four times. These f4 mice are 93.75% FVB and offspring of a cross to C57 are 46.9% FVB:53.1% C57. I am currently collecting samples at 15 and 24 weeks of age from the 46.9% FVB:53.1% C57 mice which carry the TRAMP transgene and are of four possible Dnmt1 hypomorphic phenotypes (WT, N/+, R/+, N/R). To date ~95% of these animals have been collected with approximately 20 animals per genotype for each time point. At the early time point (15 weeks of age) half of the samples have had the prostate tissue embedded for histological analysis and half have been frozen for molecular analysis as the prostate is very small at this age. At the later time point (24 weeks of age) prostate tissue was always embedded first and any remaining tissue was frozen for molecular analyses.

At the time of necropsy, several parameters were measured: palpable tumor incidence, tumor incidence, metastatic incidence, prostate weight, urogenital tract (UG) weight, and body weight. At 15 weeks of age we find that Dnmt1 hypomorphic mice tend to have increased tumor incidence compared to WT TRAMP mice, with at least twice as many animals presenting with tumor (Table 1). However, there was no change in prostate or UG weight after normalization by body weight (Fig. 3a-b). Interestingly, at 24 weeks of age there is no difference in tumor incidence, but a slight decrease in palpable tumor incidence in R/+ and N/R mice compared to WT (Table 1). However, 11-17% of R/+ and N/+ mice and 0% of N/R mice have obvious metastatic disease upon necropsy as compared to WT mice, in which approximately 32% have metastases (Table 1). Prostate weights appear to be decreased in R/+ and N/R mice compared to WT mice and UG weights in R/+ mice also show this trend (Fig. 3c-d). Although the percentages of mice displaying tumors or metastases upon necropsy clearly change in the R/+, N/+, and N/R mice compared to WT mice, the only statistically significant change was metastatic incidence in N/R mice (Table 1).

In addition to these macroscopic parameters, stage of tumor progression has also been measured microscopically with hematoxylin and eosin staining. Tissue sections were scored for tumor stage (Normal-N, Prostatic Intraepithelial Neoplasia-PIN, Well Differentiated-WD, Moderately Differentiated-MD, and Poorly Differentiated-PD) and the percent of tissue observed of each pathological stage was determined. Two slides of tissue sections 50 µM apart were analyzed for each mouse in the study at either 15 or 24 weeks of age. In order to perform statistical analyses to compare pathological grade, a Disease Score was calculated from the percent of each pathological stage determined for each lobe, which was multiplied by a linearly increasing number to represent disease progression (DS = %N(0) + %PIN(1) + %WD(2) + %MD(3) + %PD(4)). The Disease Scores were then averaged for the two slides analyzed from each mouse. This resulted in single values for each prostatic lobe for each sample, which was then compared using the Mann-Whitney test. At 15 weeks, R/+, N/+, and N/R mice all display a shift in tumor progression, with

less normal or early stage disease and more late stage disease in all four prostatic lobes (Dorsal, Lateral, Ventral, and Anterior), as compared to WT TRAMP mice (Fig. 4a-d). As has been previously reported, the most advanced disease was in the Dorsal, Lateral, and Ventral lobes and minimal progression in the Anterior lobe (Fig. 4a-d). The Disease Score analyses also suggested advanced disease progression at 15 weeks of age in TRAMP Dnmt1 hypomorphs compared to WT TRAMP mice, with significant increases in R/+, N/+, and/or N/R in all four prostatic lobes (Fig. 5a-d).

The pattern of disease progression in TRAMP Dnmt1 Hypomorphic mice at 24 weeks of age is quite complex. First, in all four prostatic lobes (Dorsal, Lateral, Ventral, and Anterior) R/+ mice have decreased percentage of late stage disease (PD and MD) and increased normal or early stage disease (N and PIN) as compared to WT mice (Fig. 6a-d). Second, N/+ mice display increased PD disease in all prostatic lobes, except anterior, as compared to WT mice (Fig. 6a-d). Finally, N/R mice tend to have increased N and PIN tissue and decreased PD disease in the Lateral and Ventral lobes compared to WT mice (Fig. 6b-c). Interestingly, N/R mice also display an increase in PD and MD disease in the Dorsal lobe and especially the Anterior lobe compared to WT mice (Fig. 6a-d). Disease Score analysis revealed that R/+ mice display a significant decrease in disease progression compared to WT mice in the Dorsal lobe, a trend toward significance in the Lateral lobe, and an overall decrease in the mean DS in all four lobes at 24 weeks (Fig. 7a-d). Although there were no significant changes, N/+ mice did display increased DS means in the Lateral and Ventral lobes as compared to WT (Fig. 10a-d). The mean DS for N/R mice were decreased in the lateral and ventral lobes with a significant increase in the Anterior lobe compared to WT mice (Fig. 7a-d). This is a unique finding as TRAMP mice rarely develop tumors or advanced disease in the Anterior lobe, indicating that DNA methylation plays a role not only the progression but the presentation of the prostatic disease in TRAMP. Overall, these data support our observations of decreased palpable tumor incidence in R/+ and N/R mice and increased incidence in N/+ mice compared to WT TRAMP mice at 24 weeks (Table 1). However, we would still like to confirm that metastatic incidence is truly decreased or non-existent in TRAMP Dnmt1 hypomorphic mice as compared to WT TRAMP mice at this time point. In order to do this, we are currently performing Tag staining of 2 sections of tissue from 15 and 24 week old mice to identify TRAMP prostate tumor cells in liver, lung, kidney, and lymph node tissues.

I next measured Dnmt1, Dnmt3a, and Dnmt3b mRNA expression, B1 repetitive element methylation, and global (5mdC) levels of methylation in the prostates of 15 and 24 week old TRAMP Dnmt1 Hypomorphic mice. Because all of these parameters become altered during TRAMP tumor progression, we were unsure of how they may change in the TRAMP Dnmt1 Hypomorphic mice (1-3). Dnmt1, Dnmt3a, and Dnmt3b mRNA expression are similar for all four genotypes at 15 weeks of age, with a slight decrease in Dnmt1 in N/R mice (Fig. 8a-c). At 24 weeks of age, Dnmt1 mRNA expression is significantly decreased in R/+ and N/R mice compared to WT TRAMP mouse prostate tissue (Fig. 8d-f). Dnmt3a and Dnmt3b mRNA expression shows some variability amongst the four genotypes with a significant increase in Dnmt3A in prostate tissue from N/+ mice (Fig. 8d-f). We have previously shown that Dnmt expression increases with tumor progression (3). Interestingly, at 15 weeks R/+, N/+, and N/R mice appear to have more advanced disease than WT mice and at 24 weeks, N/+ mice appear to have more progressive disease (Figs. 3-6). In all of these instances, Dnmt1 expression is not decreased as expected and Dnmt3A and Dnmt3B may also be increased. Therefore, I next compared Dnmt mRNA expression to stage in tumor progression. Expression of all three Dnmt genes increased with tumor progression at both 15 and 24 weeks, suggesting that the lack of decreased Dnmt1 mRNA expression and the variable mRNA expression of Dnmt3A and Dnmt3B are at least partially due to disease progression (Fig. 9a-f). B1 methylation levels are decreased in N/R mouse prostate tissue, but unchanged in R/+ and

N/+ compared to WT at both 15 and 24 weeks of age (Fig. 10a-b). Global 5mdC levels are decreased in N/R mouse prostate tissue at 15 weeks of age and N/+ and N/R mouse prostate tissue at 24 weeks of age compared to control (Fig. 10c-d). In addition, B1 methylation and 5mdC levels in prostate tissue are strongly correlative at both 15 and 24 weeks of age (Fig. 10e-f). It is possible that the progressed disease stage in N/+ mice at 24 weeks is resulting in the decreased 5mdC levels as we have previously shown that these two parameters correlate (3).

As described above, liver tissue was used as a control in the non-TRAMP Dnmt1 hypomorphic mice and we know that Dnmt expression and DNA methylation are disrupted in TRAMP tumors (1-3). Therefore we also analyzed Dnmt1, Dnmt3a, and Dnmt3b mRNA expression and B1 repetitive element methylation in liver tissue from the TRAMP Dnmt1 Hypomorpic mice at both 15 and 24 weeks of age. Dnmt1 mRNA was decreased in R/+, N/+, and N/R mice with the least Dnmt1 expression in N/R mice, as compared to WT mice at both timepoints (Fig. 11a &d). There was no change in Dnmt3A or Dnmt3b mRNA expression in the four genotypes (Fig. 11b-c & e-f). Methylation of the B1 repetitive element was decreased in both N/+ and N/R liver samples at 15 weeks and in N/R liver samples at 24 weeks as compared to WT liver samples (Fig. 12a-b). These data suggest that all three hypomorphic genotypes will result in decreased Dnmt1 mRNA levels, but that this may not necessarily result in hypomethylation of the B1 element. Overall, we confirmed the expected phenotype based on the genotype of these mice.

Currently, I am examining Dnmt1, Dnmt3A, and Dnmt3b protein expression by western blot analysis and preparing samples for HELP analyses on TRAMP Dnmt1 hypomorph prostate samples. Our goal is to identify genes that are not methylated in the Dnmt1 hypomorphic mice that normally become hypermethylated during TRAMP tumor progression. We hypothesize that these genes may be important for the progression of TRAMP tumors and especially the development of metastatic disease.

Key Research Accomplishments:

Key Scientific Findings:

- There are several genes (Mgmt, Pdlim4, Zfp185, and Glutathione-s-transferases) that are commonly hypermethylated in human prostate cancer that are also downregulated at the transcriptional level in TRAMP tumors.
- In TRAMP these genes are not regulated by DNA methylation, but perhaps some other epigenetic mechanism.
- R/+ TRAMP mice compared to WT TRAMP mice display:
    - slight increases in tumor incidence and pathological stage at 15 weeks of age
    - slight decreases in palpable tumor and metastatic incidence, as well as decreased prostate and UG weights and pathological stage at 24 weeks
    - no change in Dnmt1 mRNA expression at 15 weeks, but significantly decreased Dnmt1 mRNA expression at 24 weeks, with no change in Dnmt3a or Dnmt3b mRNA expression at either timepoint
    - no change in B1 methylation or in 5mdC levels at either time point
- N/+ TRAMP mice compared to WT TRAMP mice display:
    - no change in prostate or UG weight at 15 or 24 weeks of age
    - increased tumor incidence and pathological stage at 15 weeks of age
    - increased palpable tumor incidence and pathological stage at 24 weeks of age
    - no significant change in Dnmt expression at either time point, except an increase in Dnmt3a at 24 weeks of age
    - no change in B1 methylation at 15 or 24 weeks of age
    - no change in 5mdC levels at 15 weeks, but significant hypomethylation at 24 weeks of age
- N/R TRAMP mice compared to WT TRAMP mice display:
    - increases in tumor incidence and pathological stage at 15 weeks of age
    - slight decrease in palpable tumor and with no metastatic incidence, with a trend toward decreased prostate weight and pathological stage at 24 weeks
    - increased tumor progression at 24 weeks specifically in the anterior lobe
    - significant decrease in Dnmt1 mRNA expression at 15 and 24 weeks
    - no significant change in Dnmt3A and Dnmt3B mRNA expression at 15 and 24 weeks
    - significant decreases in B1 methylation and 5mdC levels at 15 and 24 weeks of age
- Liver samples from TRAMP Dnmt1 hypomorphic mice have significantly decreased Dnmt1 mRNA expression, no change in Dnmt3A or Dnmt3B mRNA expression and decreased methylation of B1 in N/+ and N/R mice at 15 weeks and N/R mice at 24 weeks of age.
- Dnmt1, Dnmt3A, Dnmt3B mRNA expression positively correlate with tumor progression.
- B1 methylation positively correlates with 5mdC levels.

Resources:

- Dnmt1 hypomorphic mouse colony (C57Bl/6)
- Dnmt1 hypomorphic TRAMP mouse colony (FVB)

Reportable Outcomes:

Manuscripts

Cory Mavis, **Shannon R. Morey Kinney**, Barbara A. Foster, Adam R. Karpf. Expression level and DNA methylation status of Glutathione-S-transferase genes in normal murine prostate and TRAMP tumors. *The Prostate*. In Press.

Shannon R. Morey Kinney, Dominic J. Smiraglia, Smitha R. James, Michael T. Moser, Barbara A. Foster, and Adam R. Karpf. Stage-specific alterations of Dnmt expression, DNA hyper-methylation, and DNA hypomethylation during prostate cancer progression in the TRAMP model. *Molecular Cancer Res.* 6(8) August 2008. Selected as Online First Publication.

Marta Camoriano*, **Shannon R. Morey Kinney***, Michael T. Moser, Barbara A. Foster, James L. Mohler, Donald L. Trump, Adam R. Karpf, and Dominic J. Smiraglia. Phenotype-specific CpG Island Methylation Events in a Murine Model of Prostate Cancer. *Cancer Research* 68, 4173-4182, June 1, 2008.
***Equal contribution

Presentations

Oral

1. **Shannon R. Morey Kinney**. The Effects of Genetic Reduction of Dnmt1 on TRAMP tumor progression and metastasis. Pharmacology and Therapeutics Departmental Retreat, Holiday Valley Resort and Conference Center, Ellicottville, NY, October 2008.

2. **Shannon R. Morey Kinney**, Dominic J. Smiraglia, Smitha R. James, Michael T. Moser, Barbara A. Foster, and Adam R. Karpf. Stage specific alterations of the DNA methylation pathway in a mouse model of prostate cancer. DNA Function Meeting, Roswell Park Cancer Institute, March, 2008

Poster

1. **Shannon R. Morey Kinney**, Dominic J. Smiraglia, Smitha R. James, Michael T. Moser, Barbara A. Foster, and Adam R. Karpf. Stage-specific alterations of Dnmt expression, DNA hyper-methylation, and DNA hypomethylation during prostate cancer progression in the TRAMP model. AACR Cancer Epigenetics Meeting, Boston, MA, May, 2008.

3. **Shannon R. Morey Kinney**, Marta Camoriano, Michael T. Moser, Barbara A. Foster, Dominic J. Smiraglia, and Adam R. Karpf. Restriction Landmark Genomic Scanning Reveals Phenotype Specific Epigenomic Patterns in a Mouse Model of Prostate Cancer. Annual Pharmacology Sciences Day, University at Buffalo, May, 2008.

Conclusions:

We have identified several genes that are commonly silenced in human prostate cancer through promoter hypermethylation that are also downregulated in TRAMP tumors. However, none of these genes display DNA hypermethylation in the large region of the promoter that we analyzed. Further studies suggest that epigenetic modifications, such as histone deacetylation, may still be playing a role. We have begun to use a new technique (HELP), in order to determine whether promoter methylation is a mechanism that is utilized in TRAMP tumors to silence tumor suppressor genes. This microarray based assay will cover the entire mouse genome and therefore should reveal any commonly hypermethylated promoters.

We have previously shown that global DNA hypomethylation occurs early, while locus specific DNA hypermethylation occurs late during TRAMP tumor progression. Using a Dnmt1 hypomorphic mouse model, we have tested the role of Dnmt1 and hence these DNA methylation changes in TRAMP tumorigenesis. At an early time point hypomorphic mice display advanced tumor progression and at a later time point hypomorphic mice have decreased tumor progression and metastases. First, these results suggest that global hypomethylation is an important event in prostate cancer progression and increased hypomethylation due to Dnmt1 hypomorphicity promotes that early stage event, thus pushing the progression forward. Furthermore, these data support the hypothesis that locus specific hypermethylation is repressing important tumor suppressor genes that play a role in prostate cancer progression and especially metastatic processes and decreased Dnmt1 expression prevents locus specific hypermethylation, thereby slowing or preventing these late stage processes Taken together this indicates a dual role for Dnmt1 in TRAMP tumor progression with a suppressive role in early stage disease and oncogenic role at later stages.

References:

1. Morey, S. R., Smiraglia, D. J., James, S. R., Yu, J., Moser, M. T., Foster, B. A., and Karpf, A. R. DNA methylation pathway alterations in an autochthonous murine model of prostate cancer. Cancer Res, *66:* 11659-11667, 2006.

2. Camoriano, M., Shannon R. Morey Kinney, Michael T. Moser, Barbara A. Foster, James L. Mohler, Donald L. Trump, Adam R. Karpf, and Dominic J. Smiraglia. Phenotype-specific CpG Island Methylation Events in a Murine Model of Prostate Cancer. Cancer Res, *68:* 4173-4182, 2008.

3. Morey Kinney, S. R., Dominic J. Smiraglia, Smitha R. James, Michael T. Moser, Barbara A. Foster, and Adam R. Karpf Stage-specific alterations of Dnmt expression, DNA hypermethylation, and DNA hypomethylation during prostate cancer progression in the TRAMP model. Molecular Cancer Res. 6(8) August 2008.

4. Cory Mavis, Shannon R. Morey Kinney, Barbara A. Foster, Adam R. Karpf. Expression level and DNA methylation status of Glutathione-S-transferase genes in normal murine prostate and TRAMP tumors. The Prostate. In Press.

Appendix

Supporting Data

Figure 1. Aldh1a2, Mgmt, Pdlim4, and Zfp185 mRNA expression in normal mouse prostate (N) and TRAMP prostate tumors (T). A) Aldh1a2 B) Mgmt C) Pdlim4 D) Zfp185 mRNA levels as determined by SYBR green qRT-PCR. Copy number of target genes were normalized by 18s rRNA endogenous control.

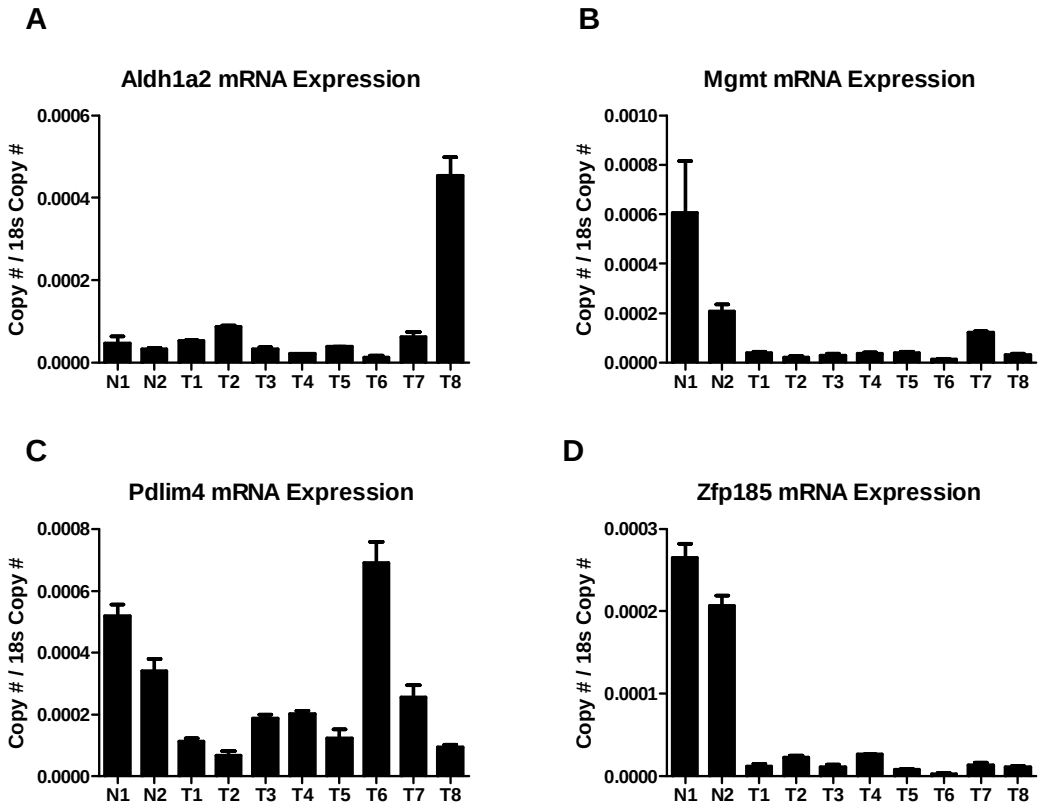

Figure 2. Mgmt, Pdlim4, and Zfp185 promoter methylation in normal mouse prostate (N) and TRAMP tumors (T). A) Mgmt B) Pdlim4 C) Zfp185 promoter methylation status as determined by traditional sodium bisulfite sequencing. Each circle represents a CpG with white circles indicating an unmethylated CpG and black circles indicating a methylated CpG. Each row of circles indicates a separate clone that was sequenced. Bent arrow indicates the transcriptional start site of the gene.

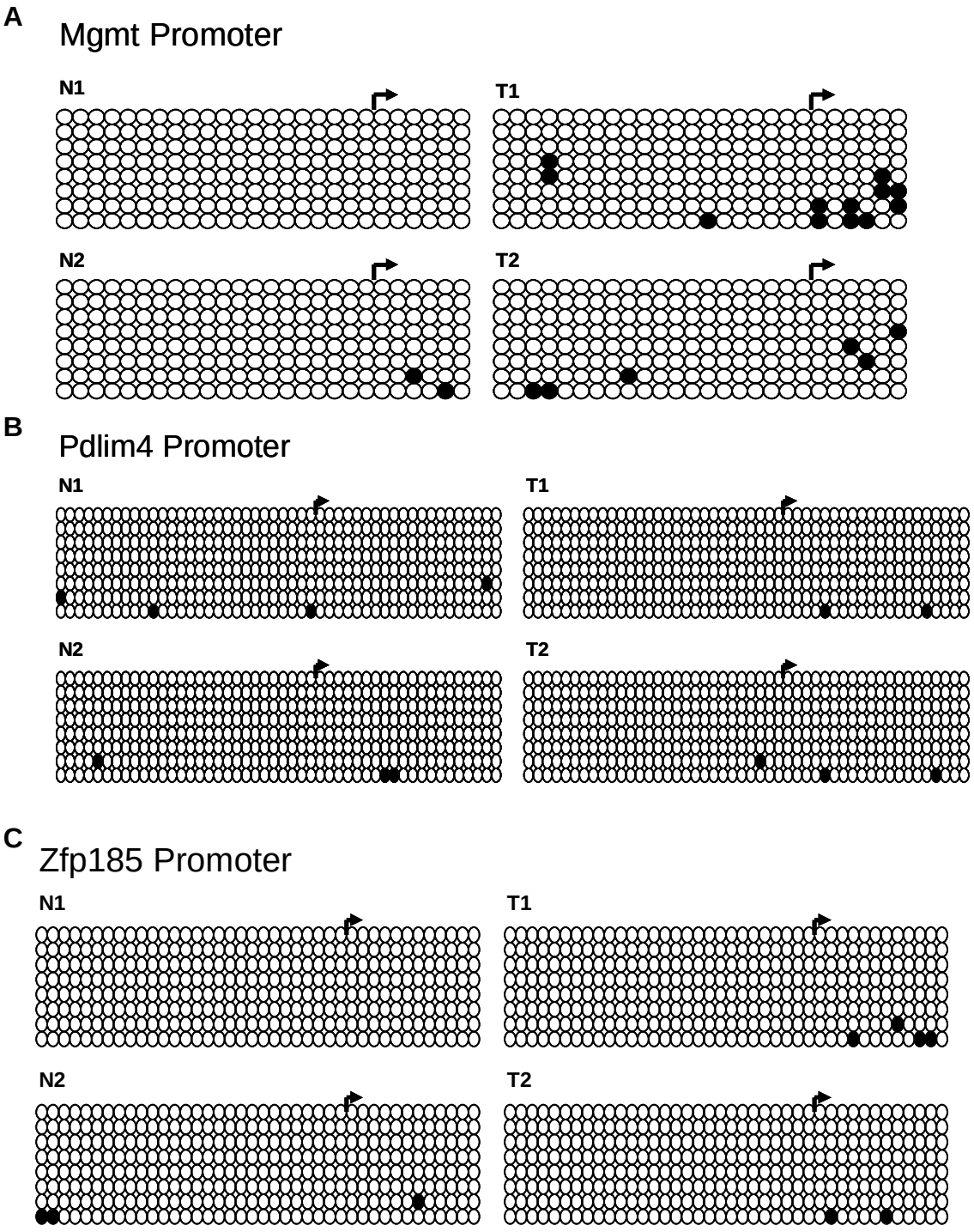

Table 1. Tumor and metastatic incidence in TRAMP Dnmt1 Hypomorphic Mice.

Genotype / Age at sac N	Tumor incidence	Fischer's Exact p-value (Vs. WT)	Palpable Tumor Incidence	Fischer's Exact p-value (Vs. WT)	Met Incidence	Fischer's Exact p-value (Vs. WT)
WT / 15 weeks	**15%**		**10%**		**5%**	
N = 20	3		2		1	
R/+ / 15 weeks	**30%**	0.47	**20%**	0.66	**0%**	1.0
N = 20	6		4		0	
N/+ / 15 weeks	**40%**	0.21	**11%**	1.0	**0%**	0.40
N = 28	11		3		0	
N/R / 15 weeks	**30%**	0.47	**10%**	1.0	**0%**	1.0
N = 20	6		2		0	
WT / 24 weeks	**89%**		**42%**		**32%**	
N = 19	17		8		6	
R/+ / 24 weeks	**74%**	0.80	**21%**	0.33	**11%**	0.26
N = 19	14		4		2	
N/+ / 24 weeks	**83%**	1.0	**54%**	0.78	**17%**	0.48
N = 24	20		13		4	
N/R / 24 weeks	**86%**	1.0	**32%**	0.76	**0%**	0.02
N = 22	19		7		0	

Figure 3. Prostate and Urogenital Tract (UG) weights normalized by body weight in TRAMP Dnmt1 Hypomorphic mice. A) Prostate weight in 15 week old TRAMP mice. B) UG weight in 15 week old TRAMP mice. C) Prostate weight in 24 week old TRAMP mice. D) UG weight in 24 week old TRAMP mice. Each symbol indicates one sample and the bar indicates the mean. P-values are the result of Mann-Whitney test statistical analyses compared to WT indicating a trend toward significance ($p \leq 0.1$).

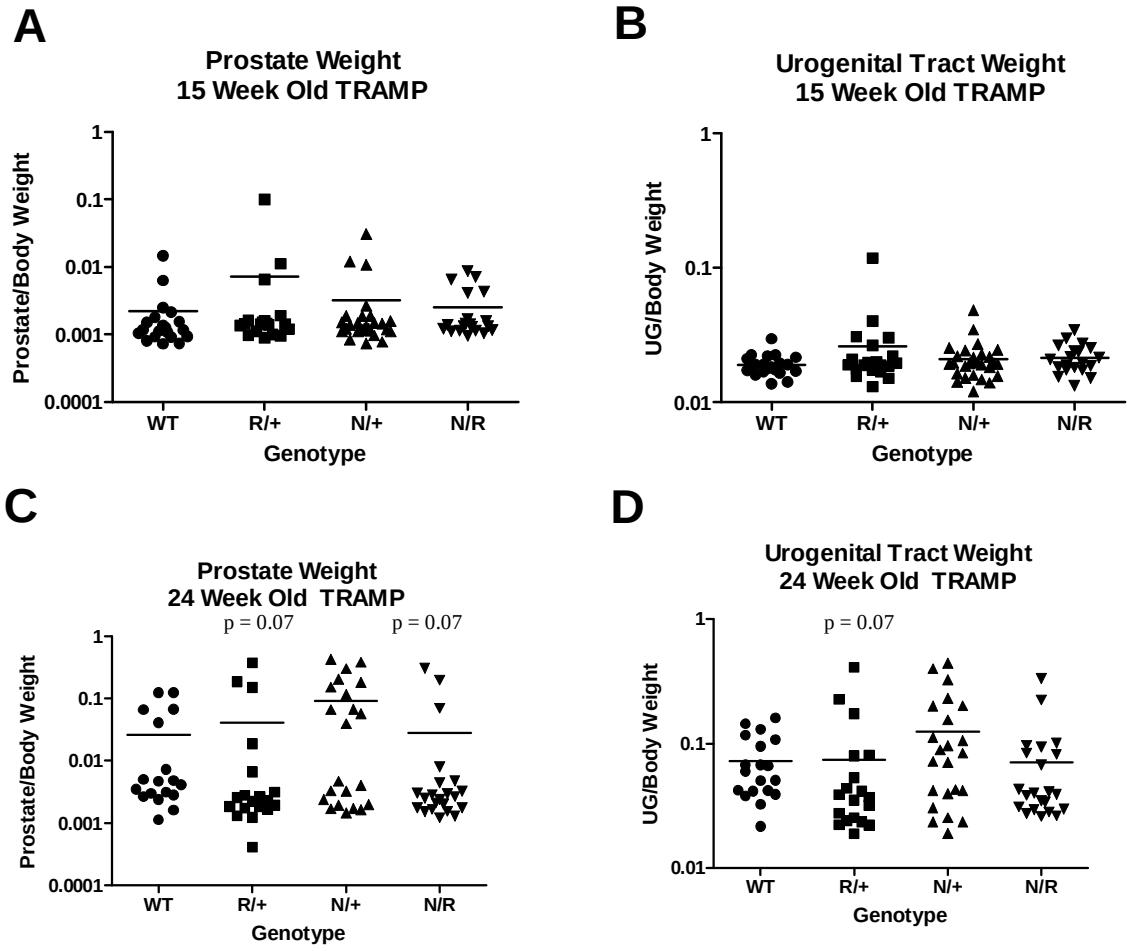

Figure 4. Histological analysis of prostate tumor stage in 15 week old TRAMP Dnmt1 Hypomorphic mice. Microscopic analysis of hematoxylin and eosin staining of prostate tissue from WT, R/+, N/+, and N/R TRAMP mice at 15 weeks of age. Percent of each pathological grade (N-Normal, PIN-Prostatic Intraepithelial Neoplasia, WD-Well Differentiated, MD-Moderately Differentiated, PD-Poorly Differentiated) was determined and averaged for all of the animals in each group for the four lobes of mouse prostate A) Dorsal, B) Lateral, C) Ventral, and D) Anterior. Two sections from the prostate of each mouse were analyzed at 40X magnification for each genotype.

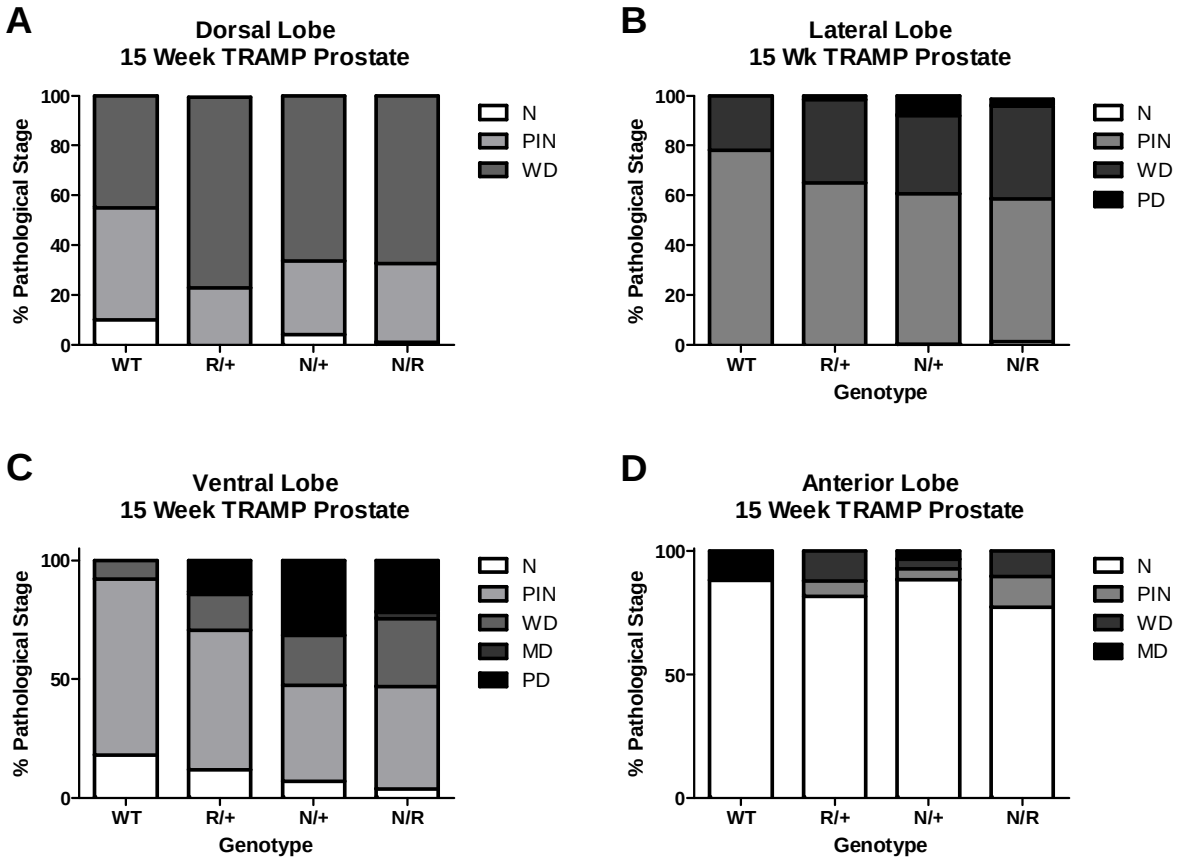

Figure 5. Prostate cancer Disease Score in 15 week old TRAMP Dnmt1 Hypomorphic mice. A) Disease Score values based on pathological grading of the A) Dorsal B) Lateral C) Ventral and D) Anterior lobes in WT, R/+, N/+, and N/R TRAMP mice at 24 weeks of age. Disease Score was calculated as described above. Each symbol represents the average of two slides examined for each mouse and the bar indicates the mean of each group. P-values are the result of Mann-Whitney test statistical analyses compared to WT indicating statistical significance ($p < 0.05$) or a trend toward significance ($p \leq 0.1$).

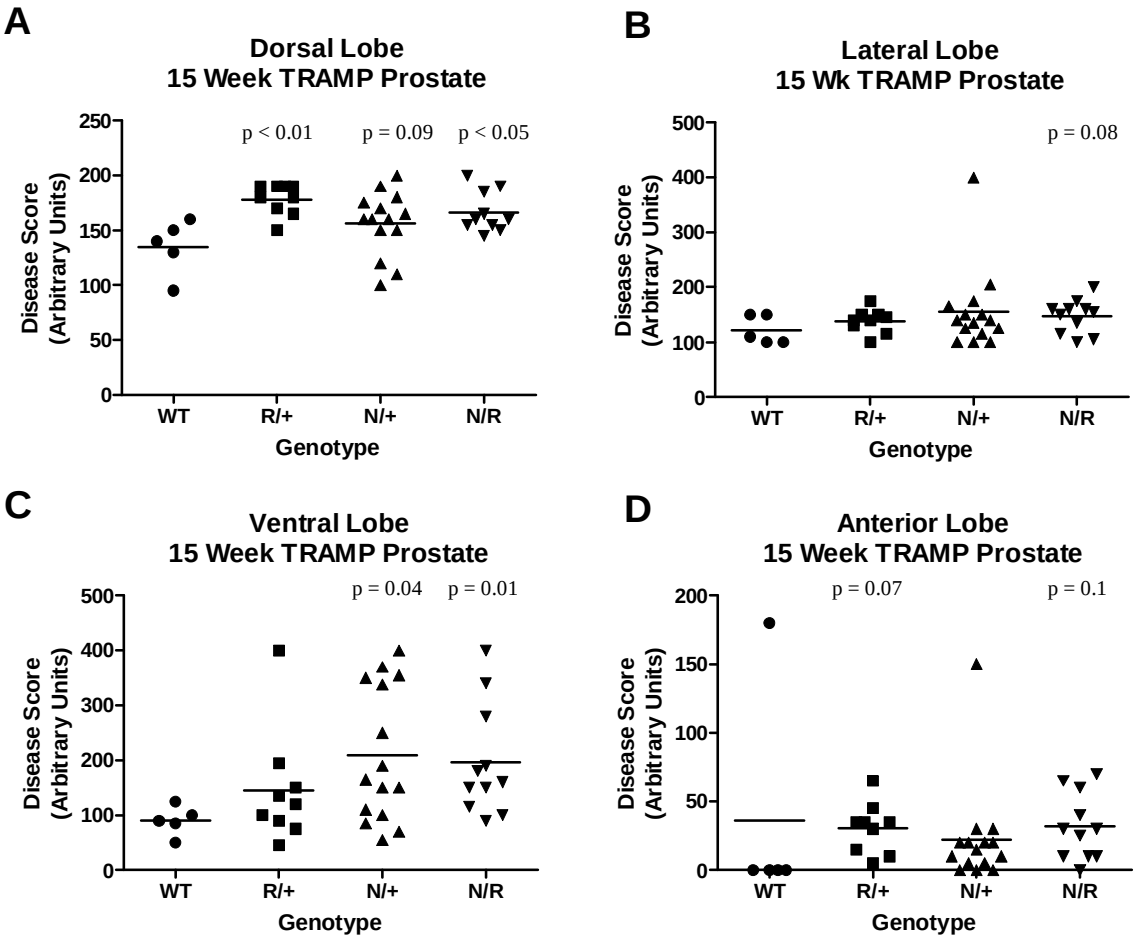

Figure 6. Histological analysis of prostate tumor stage in 24 week old TRAMP Dnmt1 Hypomorphic mice. Microscopic analysis of hematoxylin and eosin staining of prostate tissue from WT, R/+, N/+, and N/R TRAMP mice at 24 weeks of age. Percent of each pathological grade (N-Normal, PIN-Prostatic Intraepithelial Neoplasia, WD-Well Differentiated, MD-Moderately Differentiated, PD-Poorly Differentiated) was determined and averaged for all of the animals in each group for the four lobes of mouse prostate A) Dorsal, B) Lateral, C) Ventral, and D) Anterior. Two sections from the prostate of each mouse were analyzed at 40X magnification for each genotype.

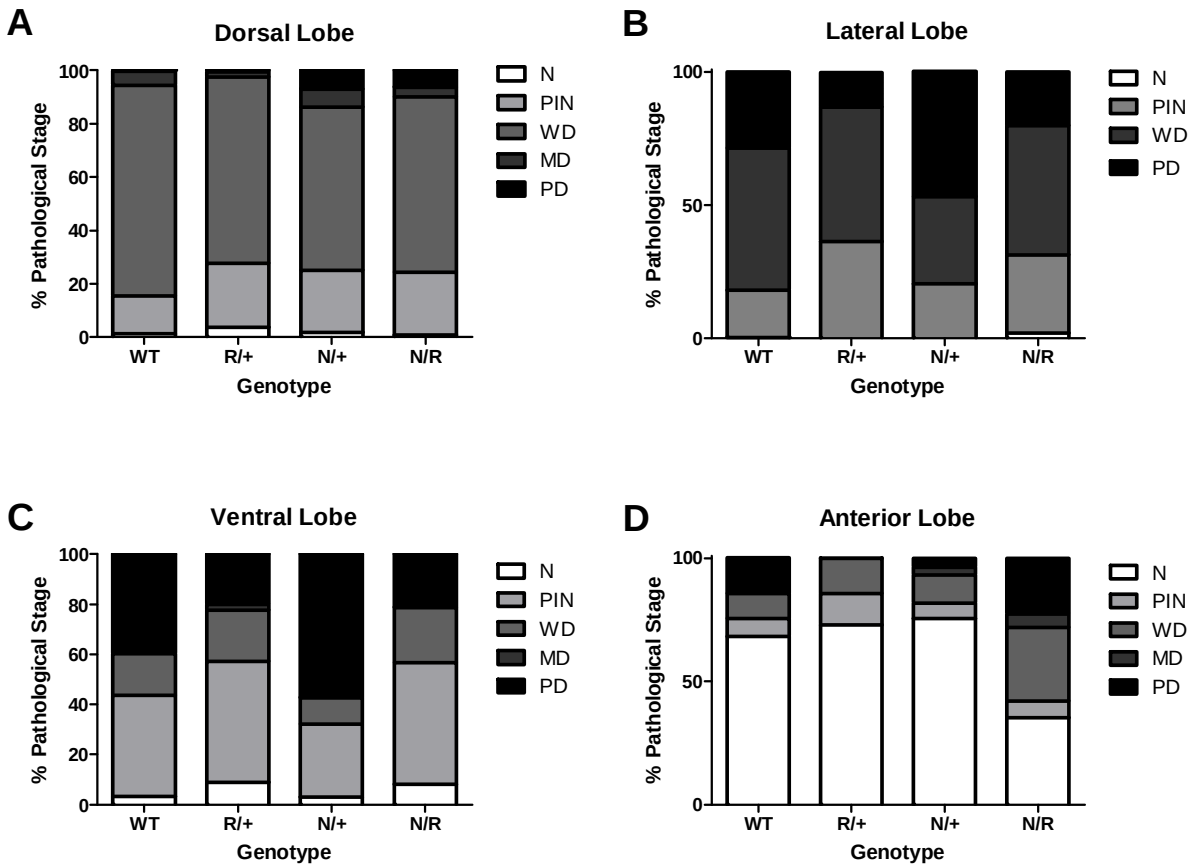

Figure 7. Prostate cancer Disease Score in 24 week old TRAMP Dnmt1 Hypomorphic mice. A) Disease Score values based on pathological grading of the A) Dorsal B) Lateral C) Ventral and D) Anterior lobes in WT, R/+, N/+, and N/R TRAMP mice at 24 weeks of age. Disease Score was calculated as described above. Each symbol represents the average of two slides examined for each mouse and the bar indicates the mean of each group. P-values are the result of Mann-Whitney test statistical analyses compared to WT indicating statistical significance ($p < 0.05$) or a trend toward significance ($p \leq 0.1$).

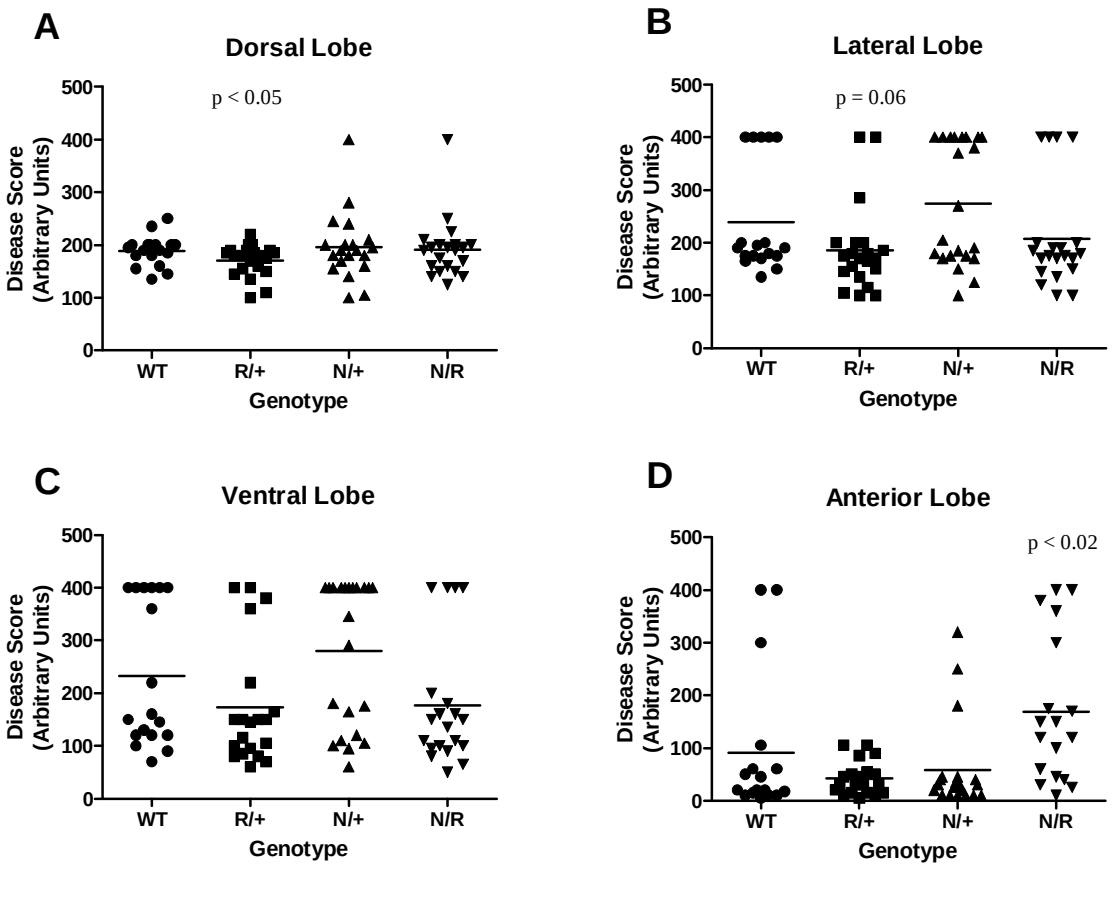

Figure 8. Dnmt1, Dnmt3a, and Dnmt3b mRNA expression in prostate tissue from TRAMP Dnmt1 Hypomorphic mice. A) Dnmt1 B) Dnmt3a C) Dnmt3b mRNA expression in 15 week old TRAMP prostate. D) Dnmt1 E) Dnmt3a F) Dnmt3b mRNA expression in 24 week old TRAMP prostate. Each symbol indicates one sample and the bar indicates the mean. P-values are the result of Mann-Whitney test statistical analyses compared to WT indicating statistical significance ($p < 0.05$).

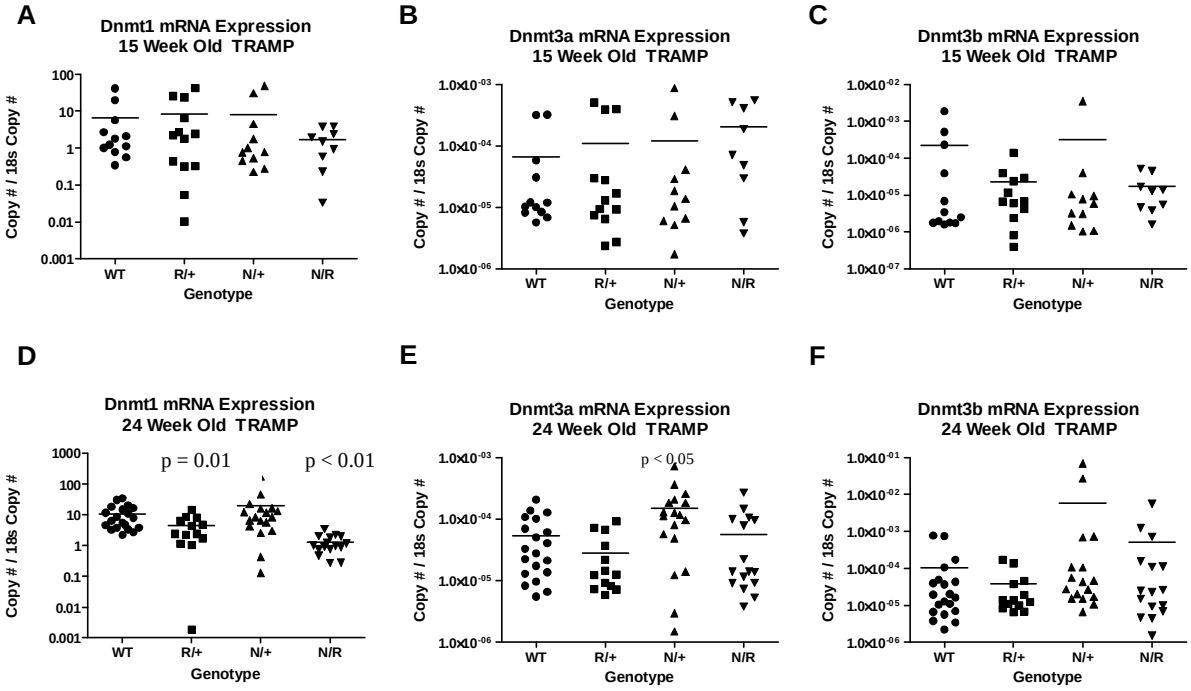

Figure 9. Dnmt1, Dnmt3a, and Dnmt3b mRNA expression increases with advanced disease in TRAMP Dnmt1 Hypomorphic mice. A) Dnmt1 B) Dnmt3a C) Dnmt3b mRNA expression in 15 week old TRAMP prostate grouped for approximate stage of disease. D) Dnmt1 E) Dnmt3a F) Dnmt3b mRNA expression in 24 week old TRAMP prostate grouped for approximate stage of disease. Each symbol indicates one sample and the bar indicates the mean.

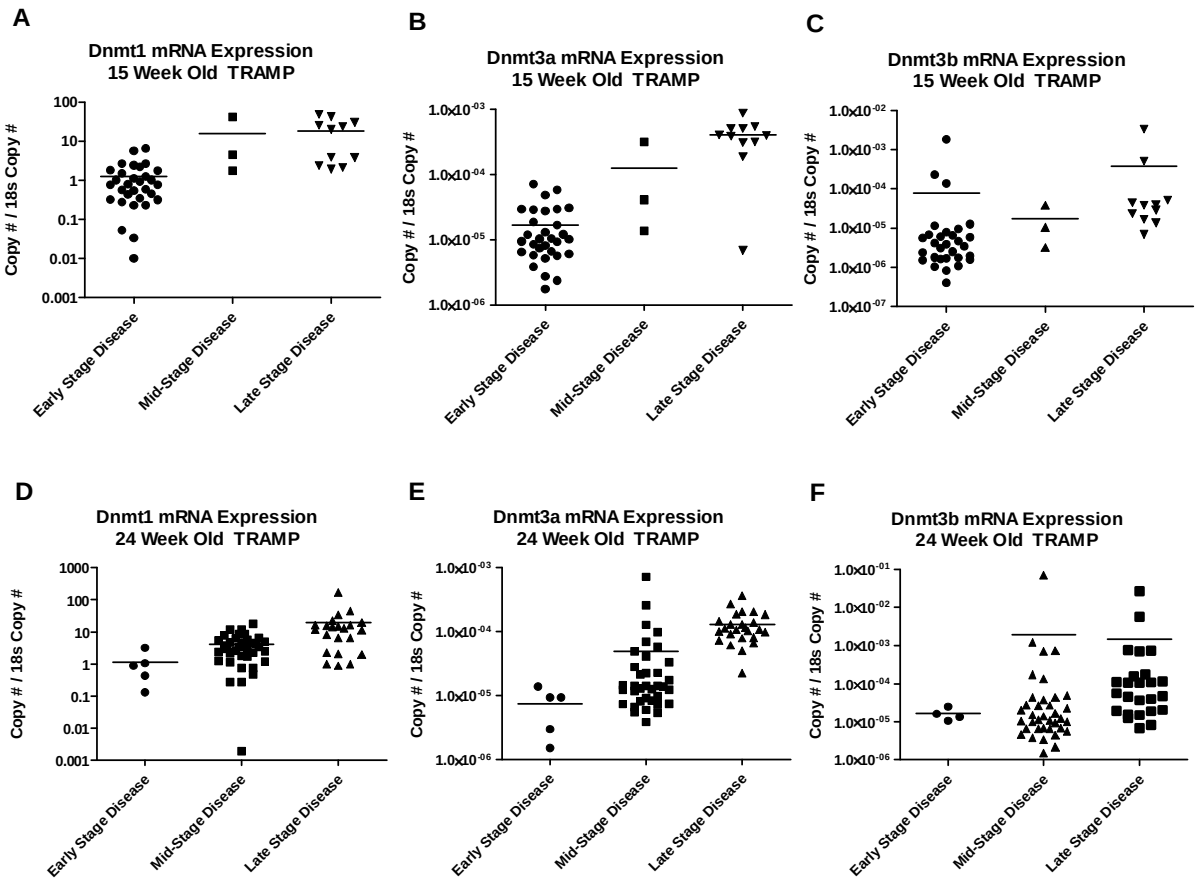

Figure 10. B1 methylation and global 5mdC levels in TRAMP Dnmt1 Hypomorphic mice. B1 methylation in A) 15 and B) 24 week old TRAMP prostate. 5mdC levels in C) 15 and D) 24 week old TRAMP prostate. Correlation analyses of B1 methylation and 5mdC levels in E) 15 and F) 24 week old TRAMP prostate. Each symbol indicates one sample and the bar indicates the mean. P-values are the result of Mann-Whitney test statistical analyses compared to WT (A-D) and Spearman correlation r and p-values (E-F). M and U are methylated and unmethylated control DNA samples.

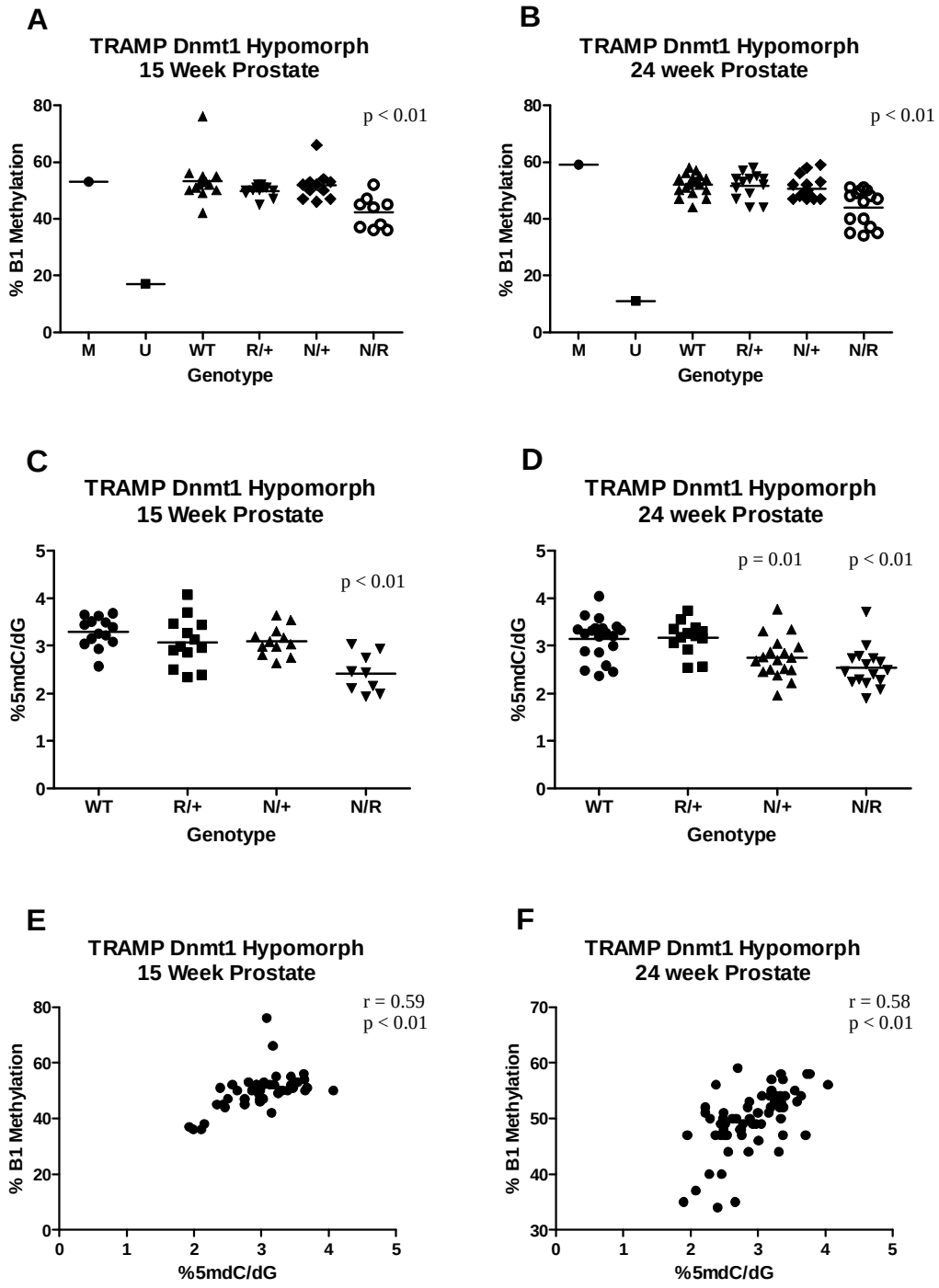

Figure 11. Dnmt1, Dnmt3a, and Dnmt3b mRNA expression in liver tissue from TRAMP Dnmt1 Hypomorphic mice. A) Dnmt1 B) Dnmt3a C) Dnmt3b mRNA expression in 15 week old TRAMP liver. D) Dnmt1 E) Dnmt3a F) Dnmt3b mRNA expression in 24 week old TRAMP liver. Each symbol indicates one sample and the bar indicates the mean. P-values are the result of Mann-Whitney test statistical analyses compared to WT indicating statistical significance ($p < 0.05$) or a trend toward significance ($p \leq 0.1$).

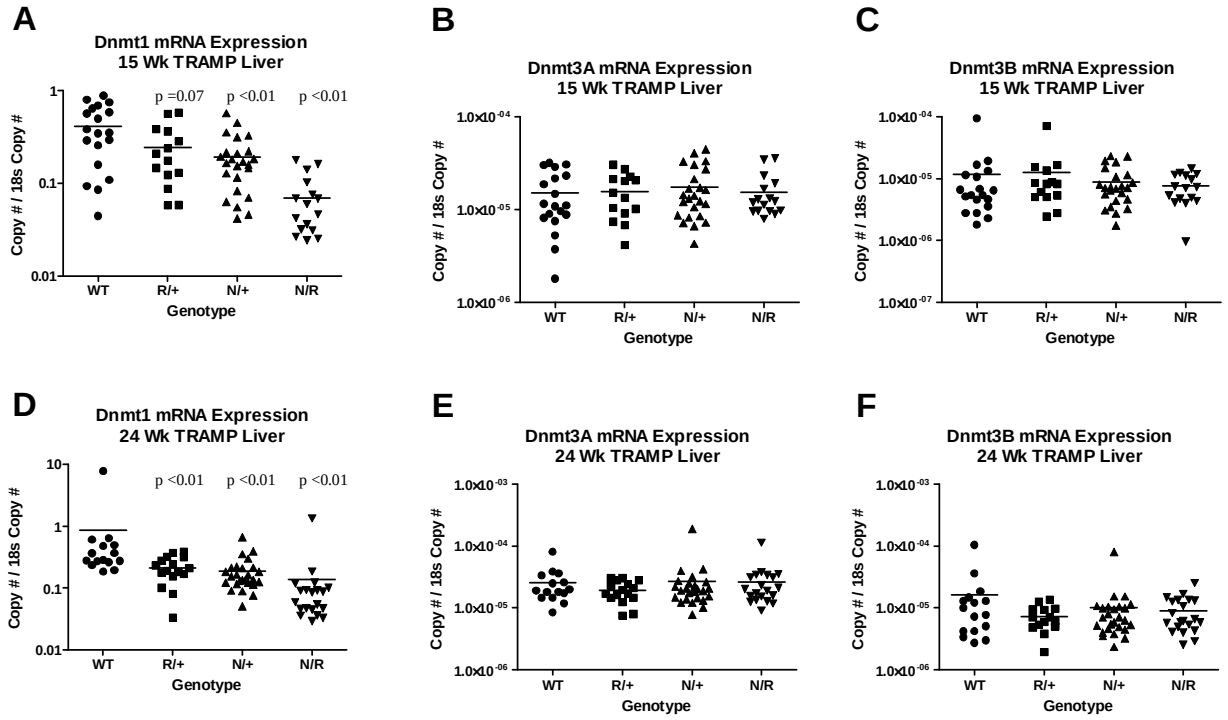

Figure 12. B1 methylation levels in TRAMP Dnmt1 Hypomorphic mice. B1 methylation in liver tissue from A) 15 and B) 24 week old TRAMP Dnmt1 Hypomorphs. Each symbol indicates one sample and the bar indicates the mean. P-values are the result of Mann-Whitney test statistical analyses compared to WT. M and U are methylated and unmethylated control DNA samples.

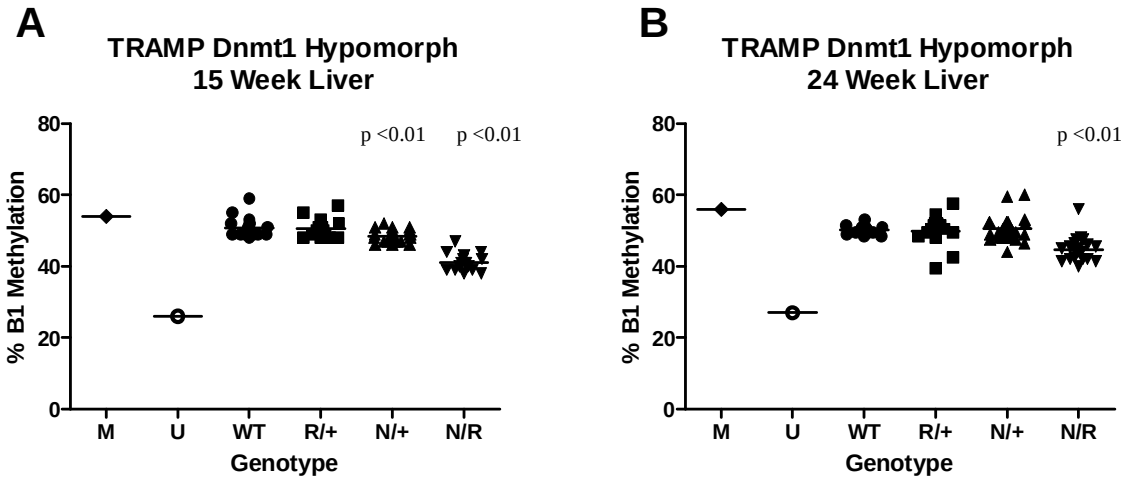

Reference 4

The Prostate

Expression level and DNA methylation status of Glutathione-S-transferase genes in normal murine prostate and TRAMP tumors

Journal:	*The Prostate*
Manuscript ID:	PROS-09-066
Wiley - Manuscript type:	Original Article
Date Submitted by the Author:	25-Feb-2009
Complete List of Authors:	Karpf, Adam; Roswell Park Cancer Institute, Pharmacology and Therapeutics Mavis, Cory; Roswell Park Cancer Institute, Pharmacology and Therapeutics Morey Kinney, Shannon; Roswell Park Cancer Institute, Pharmacology and Therapeutics Foster, Barbara; Roswell Park Cancer Institute, Pharmacology and Therapeutics
Key Words:	DNA methylation, epigenetics, Glutathione-S-transferase, TRAMP, prostate cancer

Expression level and DNA methylation status of Glutathione-S-transferase genes in normal murine prostate and TRAMP tumors

Cory K. Mavis, Shannon R. Morey Kinney, Barbara A. Foster, and Adam R. Karpf

Department of Pharmacology and Therapeutics, Roswell Park Cancer Institute, Elm and Carlton Streets, Buffalo, NY 14263

Correspondence: Dr. Adam R. Karpf, Department of Pharmacology and Therapeutics, Roswell Park Cancer Institute, Elm and Carlton Streets, Buffalo, NY 14263, Phone: 716-845-8305, Fax: 716-845-8857; e-mail: adam.karpf@roswellpark.org

Running Title: Gst gene expression and methylation in TRAMP

Keywords: DNA methylation, TRAMP, Glutathione-S-transferase, prostate cancer

Abbreviations: Gst, Murine Glutathione-S-transferase gene; TRAMP, transgenic adenocarcinoma of mouse prostate; DNMT, cytosine DNA methyltransferase.

Grant Support: NIH R21CA128062 (ARK), Roswell Park Alliance Foundation (ARK), NIH 5T32CA009072 (SRMK), DOD PC060354 (SRMK), NCI Center Grant CA16056 (Roswell Park Cancer Institute).

Disclosure Statement:

The authors declare no competing financial interests.

ABSTRACT

BACKGROUND. Glutathione-S-transferase (Gst) genes are down-regulated in human prostate cancer, and GSTP1 silencing is mediated by promoter DNA hypermethylation in this malignancy. We examined Gst gene expression and Gst promoter DNA methylation in normal murine prostates and *Transgenic Adenocarcinoma of Mouse Prostate* (TRAMP) tumors.

METHODS. Primary and metastatic tumors were obtained from TRAMP mice, and normal prostates were obtained from strain-matched WT mice (n=15/group). Quantitative real-time RT-PCR was used to measure *GstA4, GstK1, GstM1, GstO1,* and *GstP1* mRNA expression, and Western blotting and immunohistochemical staining was used to measure GstM1 and GstP1 protein expression. MassARRAY Quantitative Methylation Analysis was used to measure DNA methylation of the 5' CpG islands of *GstA4*, *GstK1*, *GstM1*, *GstO1*, and *GstP1*. TRAMP-C2 cells were treated with the epigenetic remodeling drugs decitabine and trichostatin A (TSA) alone and in combination, and *Gst* gene expression was measured.

RESULTS. Of the genes analyzed, GstM1 and GstP1 were expressed at highest levels in normal prostate. All five Gst genes showed greatly reduced expression in primary tumors compared to normal prostate, but not in tumor metastases. Gst promoter methylation was unchanged in TRAMP tumors compared to normal prostate. Combined decitabine + TSA treatment significantly enhanced the expression of 4/5 Gst genes in TRAMP-C2 cells.

CONCLUSIONS. Gst genes are extensively downregulated in primary but not metastatic TRAMP tumors. Promoter DNA hypermethylation does not appear to drive Gst gene repression in TRAMP primary tumors; however, pharmacological studies using TRAMP cells suggest the involvement of epigenetic mechanisms in Gst gene repression.

INTRODUCTION

Glutathione S-transferase (Gst) genes are phase II detoxification enzymes that detoxify xenobiotics, environmental carcinogens, and reactive oxygen species (1,2). Gst proteins catalyze the addition of reduced glutathione to substrates to form thiolethers (1,3), resulting in the formation of less toxic and reactive products that are targeted for excretion (4). Mammalian Gst enzymes are subdivided into three main groups, including a diverse family of cytosolic Gst genes including (Alpha (A) Mu (M), Pi (P), Sigma (S), Theta (T), Zeta (Z), and Omega (O), the mitochondrial GST gene Kappa (K), and microsomal Gst genes, designated MAPEG (4). Increased Gst activity is a response associated with exposure to toxic and foreign compounds and may reduce the mutagenic burden imposed by exposure to these agents (1,5). In support of this idea, GstP1/P2 knockout mice show an increased incidence of 7,12 dimethylbenz[a]anthracene (DMBA)-induced skin tumors (2). Murine tissues that are exposed to increased levels of carcinogens and xenobiotics, including liver and kidney, show higher levels of Gst expression (1). Increased levels of toxic metabolites induce Gst gene expression through the Keap1/Nrf2 pathway, which activates GST gene expression via antioxidant response element (ARE) enhancers found in Gst promoter regions (4). Consistent with this model, Nrf2 null mice display decreased basal expression of multiple Gst genes (6).

In murine chemically-induced carcinogenesis models and human cancer, Gst genes are frequently over-expressed (4,7). However, in contrast to most tumor types, GST genes are frequently down-regulated in human prostate cancer (7,8). Of particular note, GSTP1 is transcriptionally silenced by DNA hypermethylation in human prostate cancer at high frequency and consequently is being developed as a diagnostic marker for prostate cancer (9-19). GSTP1 hypermethylation is an early event during prostate cancer formation, occurring in atrophic hyperplasia and prostatic intraepithelial neoplasia. Functional loss of GSTP1 has been proposed to promote the development of genomic instability and prostate cancer (20). Recently, DNA methylation silencing of Mu-class Gst genes was reported in Barrett's adenocarcinoma, further supporting a role for DNA hypermethylation in Gst gene deregulation in human cancer (21).

DNA methylation is an epigenetic mark that regulates gene expression and plays a critical role in embryonic development, cellular differentiation, and carcinogenesis (22). Moreover, changes in DNA methylation play a key role in cancer (23). In addition to DNA methylation, histone modifications, including lysine acetylation and methylation, are epigenetic regulatory marks that are frequently altered in cancer (24). Epigenetic changes are distinct from genetic mutations in a number of respects, most consequentially in that they are reversible. This reversibility is important both from the standpoint of cancer prevention and treatment, as nutritional and pharmacological agents that prevent or reverse epigenetic gene silencing may have utility in cancer intervention strategies (25,26). In addition, the fact that epigenetic signals are reversible may serve as a mechanism whereby tumor cells can differentially regulate gene expression at distinct stages of tumorigenesis (27).

We and others have recently established *Transgenic Adenocarcinoma of Mouse Prostate* (TRAMP) as a useful *in vivo* model to interrogate the role of epigenetic alterations in prostate cancer (28-32). TRAMP utilizes expression of SV40 early genes driven by the androgen-dependent rat probasin promoter to drive prostate tumorigenesis in the mouse (33). TRAMP displays pathological stages of prostate cancer progression in a age-dependent fashion, and progresses to metastatic tumor growth similar to the human disease (34). In addition, castration of TRAMP animals results in progression to a castration-resistant disease phenotype, as is observed in humans (35). We have previously demonstrated that TRAMP mice display stage-specific alterations in DNA methyltransferase (Dnmt) protein expression, locus- and phenotype-specific DNA hypermethylation, and global DNA hypomethylation, similar to the epigenetic defects observed in human prostate cancer (28,30,31). In addition, Day and colleagues have shown that pharmacological inhibition of DNA methylation prevents prostate cancer formation, delays castration-resistant disease, and extends survival in TRAMP mice (29,32). These studies have validated TRAMP as a useful model for deciphering the contribution of aberrant DNA methylation to prostate cancer.

The goals of the current study were two-fold. First, we sought to determine Gst gene expression levels during tumor progression in TRAMP, to determine whether these genes are downregulated, as has been observed in the human disease. Second, we investigated whether promoter DNA hypermethylation is associated with the silencing of GstP1 and/or other Gst genes in TRAMP. We also utilized TRAMP cells grown *in vitro* to investigate the possibility that Gst genes are epigenetically regulated in this model. Our data indicate that Gst genes are extensively downregulated in primary tumors in the TRAMP model but that this phenotype does not correlate with DNA hypermethylation at proximal promoter regions. However, epigenetic modulatory drugs used in combination led to the activation of specific Gst genes in TRAMP cells, suggesting that additional epigenetic mechanisms beyond DNA methylation likely play a role in Gst gene repression in TRAMP.

MATERIALS AND METHODS

Animals and Tissue Samples

TRAMP 50:50 C57BL/6 x FVB and strain-matched wild-type (WT) animals and tissues have been described previously (31). Samples used in the current study are listed in Table 1. DNA was extracted from 40 mg tissue samples using the Puregene genomic DNA extraction kit (Gentra Systems, Minneapolis, MN). RNA was extracted from 20 mg tissue samples using Trizol (Invitrogen, Carlsbad, CA). Cytosolic protein was extracted from 40 mg tissue samples using the NE-PER Kit (Pierce, Rockford, IL).

Quantitative Real-Time Reverse Transcriptase PCR (qRT-PCR)

qRT-PCR was performed using the 7300 Real-time PCR system (Applied Biosystems, Foster City, CA) as described previously (31), except that absolute quantification of mRNA copy number relative to 18s rRNA was used. Gene-specific *Gst* primers are listed in Supplemental Table 1. Primers for 18s rRNA were described previously (36).

Western Blotting

Western blotting was performed as described previously (31). 20 µg cytosolic protein extracts were loaded per lane. Membranes were probed with the rabbit anti-GstM1 (1:1000) (Upstate Biotechnology, Lake Placid, NY) or polyclonal rabbit anti-GstP1 (1:1500) (MBL laboratories, Naka-ku Nagoya, Japan), followed by donkey anti-rabbit secondary antibody (Amersham Biosciences, Buckinghamshire, England). Band density was quantified using the Versa Doc 5000 Imager System and Quantity One software (BioRad, Hercules, CA) as described (31).

Immunohistochemistry (IHC)

IHC was performed on 5µm sections from paraffin embedded samples of normal prostates from WT mice and primary TRAMP tumors using standard methods. Briefly, endogenous peroxidase was blocked for 15 min at room temperature, using 3% H_20_2 in methanol. Antigen was retrieved by boiling the slides in Citrate buffer for 20 min. Slides were placed in a humidified chamber with 300µl of 1°

polyclonal anti-GstP1 antibody (rabbit 1:2000) or GstM1 1° polyclonal antibody (1:300), diluted in 1% BSA/1X Tris-$P0_4$, and incubated overnight at 4ºC. Next, slides were incubated with secondary antibody (donkey α-rabbit (1:100) secondary antibody (Amersham) at room temperature for 2 hrs. Images of representative tissues were obtained using an Olympus IX50 inverted Microscope and Retiga EXi Camera.

MassARRAY Quantitative DNA Methylation Analyses (MAQMA)

MAQMA is a quantitative assay that utilizes matrix-assisted laser desorption/ionization (MALDI) time of flight (TOF) mass spectrometry (MS) and base-specific cleavage to interrogate DNA methylation patterns in sodium-bisulfite converted DNA (37). Primers used for MAQMA analysis are shown in Supplemental Table 1. Sodium bisulfite conversions were accomplished using the EZ DNA methylation kit (Zymo Research, Orange, CA), and DNA methylation analysis was performed using the MassARRAY system and EpiTYPER software (Sequenom, San Diego, CA). Assay controls included DNA from disease-free mouse whole blood (Clontech, Cat.# 6650-1) as unmethylated control, this same DNA methylated to completion *in vitro* using SssI CpG methylase (New England Biolabs, Beverly, MA) as methylated control, and a 50:50 mix of the unmethylated and methylated control DNAs.

TRAMP-C2 Cells and Drug Treatments

The TRAMP-C2 cell line and its *in vitro* cultivation conditions were described previously (38). Briefly, cells were grown in DMEM media with 10% FBS, 5 ug/ml insulin, 50 units/ml pen-strep, 2 mM L-glutamine, and 10^{-8} M DHT. Cells were treated with 5-aza-2'-deoxycytidine (decitabine) (Sigma, St. Louis, MO) dissolved in PBS and/or Trichostatin A (TSA) (Sigma) solubilized in DMSO. Cells were treated with 1.0 μM decitabine on day 0 and day 2. On day 4, cells were treated with 600 nM TSA or DMSO control. Cells were harvested on day 5. For TSA-only treatments, cells were treated with 600 nM TSA and harvested one-day (24 hours) post treatment. RNAs were extracted and qRT-PCR analyses for Gst gene expression were performed as described above.

RESULTS

Gst mRNA Expression in Normal Mouse Prostate and TRAMP tumors

We initially sought to determine the expression patterns of various Gst genes at the mRNA level in normal murine prostate and TRAMP tumors. Of note, a recent study reported that Gst-M genes are downregulated in TRAMP (39), but the expression levels of other Gst family members in TRAMP are unknown, as are the level of expression of different Gst genes in normal murine prostate. To address these questions, we developed quantitative real time RT-PCR (qRT-PCR) assays to measure the expression of five Gst genes: *GstA4*, *GstK1*, *GstM1*, *GstO1*, and *GstP1* (Supplemental Table 1). We chose to focus on these five Gst genes because GSTP1 silencing is well established in human prostate cancer (12), and a recent microarray study indicated potentially reduced expression of these particular Gst genes in T-antigen induced murine tumors ((40) and K.K. Deeb, personal communication). The tissues under study included 15 primary and 15 metastatic tumors from TRAMP animals as well as 15 normal prostates from strain-matched WT animals (Table 1). For the metastatic tumors, we utilized five samples each from kidney, liver, and lymph node metastases (Table 1). For all parameters measured in this study, we obtained virtually identical results for the three different metastatic sites (data not shown), thus these data are combined together into one group in the graphs presented below.

qRT-PCR analysis revealed the relative expression of the five *Gst* genes in normal prostate as *GstM1>>GstP1>GstO1>GstK1>GstA4* (Fig 1A). This finding suggests a more prominent role for GstM1 (and to a lesser extent GstP1) in the function of the normal murine prostate as compared to the other Gst genes. We next examined *Gst* gene expression in TRAMP primary and metastatic tumors. Strikingly, we observed a similar pattern of expression of each *Gst* gene, with significantly reduced expression in primary tumors, and increased expression (relative to primary tumors and/or normal prostates) in metastatic tumors (Fig. 1B-F). This general pattern held true despite the differences in the basal level of expression of each gene in the normal prostate (Fig. 1A). The uniformly reduced expression of *Gst* genes in TRAMP primary tumors is clearly not an artifact of overall gene expression

levels in TRAMP, as our previous studies have demonstrated both increased and decreased expression of genes in TRAMP tumors relative to strain-matched normal prostate in this sample set (30,31).

GstM1 and GstP1 Protein Expression in Normal Mouse Prostate and TRAMP tumors

Based on the data presented above, we performed Western blot analysis to measure the expression of Gst proteins in normal prostate and TRAMP tumors. We focused our attention on GstM1 and GstP1, as antibodies from these proteins were commercially available and because these two genes displayed the highest level of mRNA expression in normal murine prostate. Additionally, GstP1 was of particular interest because it is silenced by DNA hypermethylation in human prostate cancer (12). At the mRNA level, both GstM1 and GstP1 are significantly down-regulated in primary TRAMP tumors but not in metastases (Fig. 1). Fig. 2A-B show results from Western blot analyses of GstM1 and GstP1 protein expression, respectively. As shown, GstM1 and GstP1 are expressed at high levels in normal prostate, and their expression is reduced in primary tumors (Fig. 2A-B). In metastases, GstM1 remains expressed at a lower level than normal prostate, but not as low as seen in primary tumors (Fig. 2A). In contrast, GstP1 does not show reduced protein expression in metastases, and expression is enhanced in some lesions (Fig. 2B).

To confirm our Western blot results, we performed immunohistochemical (IHC) staining of GstM1 and GstP1 in five primary TRAMP tumors along with five strain-matched normal prostates from WT mice. Representative results are shown in Supplemental Fig. 1. Negative control IgG staining of normal ventral prostate showed nuclear hematoxylin staining, but no non-specific staining (Supplemental Fig. 1A-B). In normal ventral prostate both GstM1 and GstP1 were expressed at high level in epithelial cells, with little staining in the stroma (Supplemental Fig. 1A-B). In contrast, TRAMP ventral prostate tumors showed very little staining of either protein (Supplemental Fig. 1A-B). Lateral, dorsal, and anterior prostatic lobes of TRAMP tumors were also examined and these gave similar results (data not shown). We also performed staining on a small set of metastatic tumors and observed variable GstM1

and GstP1 expression, similar to that observed for TRAMP metastases at the mRNA level and by Western blotting (data not shown). Taken together the data indicate that, similar to their mRNAs, GstM1 and GstP1 protein expression is downregulated in primary TRAMP tumors but not in tumor metastases.

DNA Methylation Status of Gst Genes in Normal Mouse Prostate and TRAMP tumors

The data presented above demonstrate that Gst gene expression is highly reduced in TRAMP primary tumors relative to normal murine prostate. GstP1 silencing is the most commonly observed hypermethylation event in human prostate cancer (41). We thus sought to determine whether DNA hypermethylation plays a role in down-regulation of GstP1 and/or other murine Gst genes in TRAMP. Initially, we analyzed the 5' regions of each Gst gene under study, as genes targeted by DNA hypermethylation in cancer contain 5' CpG islands (42). Notably, each Gst gene examined contained a 5' CpG island flanking or upstream of the predicted transcriptional start site (Fig. 3). Based on this finding, we next examined the methylation status of each gene. Given the large number of samples involved in this study (i.e. 45 biological samples x 5 genes = 225 samples for analysis), we sought a high-throughput and quantitative method for measurement of DNA methylation. For this task, we utilized MassARRAY Quantitative DNA Methylation Analyses (MAQMA) (37). MAQMA allows for quantitative measurement of DNA methylation at CpG sites contained within PCR amplicons from sodium bisulfite converted DNA. MAQMA data can be represented both as the methylation level of individual CpG sites and as the average methylation level over an entire sequenced region.

In normal murine prostate, all five Gst genes displayed a low to moderate level of DNA methylation overall, ranging from 20-40% methylation over the sequenced region (Fig 4A). For each gene, there was some variability in the methylation level of individual CpG sites within the sequenced region (Fig. 5). Based on the distinct levels of expression of the different Gst genes in normal prostate (Fig. 1A), we examined whether there is an association between Gst gene expression and Gst gene methylation levels in normal prostate. Interestingly, we observed an inverse association between

expression and methylation, although GstA4 (which shows the lowest expression in normal prostate) is an outlier (Fig. 4B). When GstA4 is removed from the data set, the correlation coefficient for the inverse association between Gst expression and methylation approaches 1.0 (Fig. 4C). These data suggest that DNA methylation could play a role in regulating Gst gene expression in normal murine prostate tissue although other factors are likely involved.

We also examined Gst promoter methylation in TRAMP tumors. Contrary to our expectation, the overall methylation level of each Gst gene was unchanged in primary tumors and metastases compared to normal prostate (Fig. 6). Despite a lack of overall methylation changes in the 5' CpG islands, hypermethylation of specific critical CpG sites could potentially account for reduced Gst gene expression in primary TRAMP tumors. To test this, we examined the methylation status of individual CpG sites within each promoter region (Fig. 5). For GstA4, two specific CpG sites (site 12 and site 16) showed increased methylation in primary tumors and metastases compared to normal prostate (Fig. 5A). However, as *GstA4* showed reduced expression in primary tumors but increased expression in metastatic tumors relative to normal prostate (Fig. 1B), it is unlikely that the methylation of these sites mediate repression. Importantly, for the other four Gst genes studied, none of the individual CpG sites showed significant methylation differences in TRAMP primary tumors relative to normal prostate from WT mice (Fig. 5B-E).

Pharmacological Inhibition of Epigenetic Enzymes induces Gst gene expression in TRAMP-C2 Cells

While the above data suggested that DNA hypermethylation may not be responsible for the repression of Gst genes in primary TRAMP tumors, we can not exclude the possibility that other epigenetic mechanisms e.g. histone deacetylation could contribute to Gst gene silencing in TRAMP and/or that DNA hypermethylation at cryptic enhancer regions could play a role. Thus, to more comprehensively test potential epigenetic repression of Gst gene in TRAMP, we utilized a

pharmacological approach on TRAMP-C2 cells grown *in vitro*. The TRAMP-C2 cell line was established from a primary TRAMP tumor obtained from a 32 week old mouse (38). MAQMA analysis of Gst gene methylation in TRAMP-C2 cells revealed that Gst genes are heterogeneously methylated, similar to that observed in normal prostate and TRAMP tumor samples (data not shown). We treated TRAMP-C2 cells with decitabine, a classical DNA methyltransferase inhibitor (43), and/or TSA, a potent histone deacetylase inhibitor (44) to test the involvement of the respective epigenetic enzymes in Gst gene expression. As shown in Fig. 7, either decitabine or TSA treatment alone did not significantly induce the expression of any of five Gst genes under study, other than a small level of induction of GstA4 with TSA, and a small level of induction of GstO1 with decitabine, respectively. In contrast, combined decitabine + TSA treatment led to significant activation of each Gst gene with the exception of GstM1 (Fig. 7). These data suggest that multiple levels of epigenetic repression are operative on Gst family genes in TRAMP.

DISCUSSION

Here we report the expression and methylation status of Gst genes in a normal murine prostate and murine prostate tumors arising in the TRAMP model. The Gst genes we studied represent 5 key Gst gene classes, including cytosolic (GstA4, GstM1, GstO1, GstP1) and mitochondrial (GstK1) class Gst genes. Of these genes, GstM1 is expressed at the highest levels in normal murine prostate, followed by GstP1. Using quantitative methods to measure gene expression and promoter DNA methylation, we find that, with the exception of GstA4, there is a strong inverse correlation between Gst gene expression and DNA methylation levels in the normal murine prostate. Most notably, we find that the expression of all five Gst genes studied is dramatically reduced at the mRNA level in primary TRAMP tumors relative to normal prostate. For GstM1 and GstP1, this observation was substantiated at the protein level using both Western blot analyses and IHC.

In contrast to the uniform Gst gene repression observed in primary TRAMP tumors, metastatic TRAMP tumors from three distinct sites (lymph node, liver and kidney) displayed variable levels of Gst gene expression relative to normal prostate, ranging from moderately reduced expression (GstK1) to dramatically increased expression (GstA4). Notably, each Gst gene was expressed at significantly higher levels in tumor metastases relative to primary tumors. We also find that promoter DNA methylation levels of each Gst gene are moderate (~20-40% methylation) in normal prostate and this value was unchanged in TRAMP tumors (either primary or metastatic). This suggests that DNA hypermethylation of Gst genes may not play a primary role in the dramatic repression of these genes observed in primary TRAMP tumors. Importantly, a lack of promoter hypermethylation of Gst genes in primary tumors along with the increased Gst gene expression in metastases may be related. It is possible that DNA hypermethylation, a relatively stable epigenetic lesion, would not be selected for as a chief mechanism for Gst gene repression in primary tumors if enhanced expression of these genes contributes to the transition to metastatic tumor growth.

Our findings of reduced Gst mRNA and protein expression in TRAMP are in agreement with a recent report that the expression of GstM genes and overall Gst enzymatic activity is decreased in TRAMP tumors (39). The fact that Gst genes of numerous classes are repressed in TRAMP tumors suggests the existence of a common underlying mechanism for repression. In this context, a key upstream regulator of Gst genes, Nrf2, is downregulated in TRAMP tumors (39). Prostate epithelial cells derived from Nrf2 null mice were shown to display reduced expression of GstM genes, overall Gst activity, and increased reactive oxygen species relative to control cells (39). Importantly, Nrf2 and GstM expression has been identified to be downregulated in human prostate cancers in microarray studies (39). The mechanism of downregulation of Nrf2 in human prostate cancer and TRAMP is currently unknown, but Frohlich et al reported that the Nrf2 gene is not DNA hypermethylated in TRAMP (39).

Nrf2 regulates Gst gene expression via binding to the antioxidant response element (ARE) found in the promoter or enhancer regions of many Gst genes (4). For the genes investigated in the current study, characterized or non-characterized ARE elements are found in the upstream promoter regions of GstA4, GstM1, and GstP1 (4). For GstA4 and GstP1, the position of the ARE is contained within the region of DNA methylation analysis. Thus although DNA hypermethylation and associated chromatin conformation changes could in theory restrict binding of Nrf2 to hypermethylated Gst promoters, this does not appear to be the mechanism of Gst downregulation in TRAMP tumors. We cannot exclude the possibility that hypermethylation of other upstream regions or cryptic enhancers of Gst genes could contribute to Gst repression in TRAMP. It also remains plausible that other epigenetic changes, e.g. histone modification status, could be altered at Gst ARE sites in TRAMP tumors. Supporting this idea, we find that combined treatment of cultured TRAMP cells with decitabine and TSA induces the expression of multiple Gst genes. Synergistic induction of epigenetically repressed genes by combined treatment with DNMT and HDAC inhibitors is a classical observation, and was noted recently for human GST-M genes (21,45). Chromatin immunoprecipitation analysis of TRAMP tissue samples, while

technically challenging, will be required to directly address the involvement of altered histone modifications in Gst gene silencing *in vivo*.

Our finding of an inverse relationship between Gst gene expression and Gst promoter DNA methylation levels in normal murine prostate was unexpected. Whether differential DNA methylation plays a role in regulating gene expression in normal tissues has been actively debated. Interestingly, recent reports have found clear evidence for this phenomenon (46-48). Moreover, a recent study found a significant inverse correlation between human *GSTM5* expression and promoter DNA methylation in normal esophageal mucosa (21). Taken together, these data suggest that DNA methylation may play a role in regulating Gst gene expression in normal tissues. Unlike normal prostate, we did not observe a clear correlation between Gst gene expression in TRAMP tumors and DNA methylation levels (data not shown).

In summary, we demonstrate that reduced Gst gene expression is a common event in primary tumors arising in the TRAMP model, reminiscent of human prostate cancer. Data presented in the current paper as well as other published work suggest a key role for oxidative stress in promoting prostate cancer in TRAMP (39,49). It appears plausible that Nrf2 and Gst gene downregulation plays a major role in the accumulation of oxidative stress in both human and murine prostate cancer. However, in contrast to the human disease, transcriptional silencing of Gst genes does not appear to involve promoter DNA hypermethylation in murine prostate cancer, at least in the TRAMP model, but may involve histone-mediated epigenetic mechanisms, including histone deacetylation. A lack of Gst gene promoter DNA hypermethylation, a relatively stable epigenetic lesion, in primary TRAMP tumors, could be related to the fact that Gst gene expression may need to be reactivated later during tumor progression in order contribute to metastatic tumor growth. Based on our work, further study of the mechanisms involved in Gst gene repression in TRAMP primary tumors, as well as direct assessment of the role of Gst gene downregulation in prostate cancer etiology are warranted.

CONCLUSIONS

Gst genes encode phase II detoxification enzymes that protect the genome from oxidative stress induced DNA damage. Unlike most malignancies, downregulation of Gst genes occurs in human prostate cancer and for at least one of these genes (GSTP1), the mechanism of this repression is promoter DNA hypermethylation. We show here that Gst genes from multiple distinct families are repressed in the TRAMP murine prostate cancer model. This repression occurs uniformly in primary TRAMP tumors, but not in tumor metastases taken from three distinct sites. Unlike human prostate cancer, GstP1 and other Gst genes do not shown proximal promoter DNA hypermethylation in either primary or metastatic murine TRAMP tumors. Data from pharmacological experiments using TRAMP cells grown *in vitro* suggest that epigenetic mechanisms in addition to DNA methylation may be involved in Gst gene repression in TRAMP. Taken together, these data suggest that Gst gene downregulation is a common etiological factor in prostate cancer and suggest TRAMP as a useful model to interrogate the role of Gst genes in prostate cancer. While the precise mechanisms leading to Gst downregulation may be distinct in human prostate cancer and TRAMP, in both circumstances it is likely that epigenetic regulatory mechanisms are involved.

ACKNOWLEDGMENTS

We are grateful to Kristin Deeb for sharing data prior to publication. We thank Mike Moser, Ellen Karasik, and Bryan Gillard of the RPCI Mouse Tumor Model Resource for assistance with the TRAMP model, Jeff Conroy and Michael Bianchi of the RPCI Microarray and Genomics Resource for assistance with MAMQA analysis, and Petra Link of the Karpf laboratory for assistance with qRT-PCR.

REFERENCES

1. Hayes JD, Pulford DJ. The glutathione S-transferase supergene family: regulation of GST and the contribution of the isoenzymes to cancer chemoprotection and drug resistance. Crit Rev Biochem Mol Biol 1995;30(6):445-600.
2. Herderson CJ, Smith IR, Rushmore TH, Crane TL, Thorn C, Kocal TE, Ferguson HW. Increased skin tumorigenesis in mice lacking pi class glutathione S-transferases. Proc Natl Acad Sci 1998;95:5275-5280.
3. Rushmore TH, Pickett CB. Glutathione S-transferases, structure, regulation, and therapeutic implications. J Biol Chem 1993;268(16):11475-11478.
4. Hayes JD, Flanagan JU, Jowsey IR. Glutathione transferases. Annu Rev Pharmacol Toxicol 2005;45:51-88.
5. Bostwick DG, Burke HB, Djakiew D, Euling S, Ho SM, Landolph J, Morrison H, Sonawane B, Shifflett T, Waters DJ, Timms B. Human prostate cancer risk factors. Cancer 2004;101(10 Suppl):2371-2490.
6. Hayes JD, Chanas SA, Henderson CJ, McMahon M, Sun C, Moffat GJ, Wolf CR, Yamamoto M. The Nrf2 transcription factor contributes both to the basal expression of glutathione S-transferases in mouse liver and to their induction by the chemopreventive synthetic antioxidants, butylated hydroxyanisole and ethoxyquin. Biochemical Society transactions 2000;28(2):33-41.
7. Bostwick DG, Meiers I, Shanks JH. Glutathione S-transferase: differential expression of alpha, mu, and pi isoenzymes in benign prostate, prostatic intraepithelial neoplasia, and prostatic adenocarcinoma. Human pathology 2007;38(9):1394-1401.
8. Nakayama M, Gonzalgo ML, Yegnasubramanian S, Lin X, De Marzo AM, Nelson WG. GSTP1 CpG island hypermethylation as a molecular biomarker for prostate cancer. Journal of cellular biochemistry 2004;91(3):540-552.
9. Lee WH, Morton RA, Epstein JI, Brooks JD, Campbell PA, Bova GS, Hsieh WS, Isaacs WB, Nelson WG. Cytidine methylation of regulatory sequences near the pi-class glutathione S-transferase gene accompanies human prostatic carcinogenesis. Proc Natl Acad Sci U S A 1994;91(24):11733-11737.
10. Li LC, Carroll PR, Dahiya R. Epigenetic changes in prostate cancer: implication for diagnosis and treatment. J Natl Cancer Inst 2005;97(2):103-115.
11. Papadopoulou E, Davilas E, Sotiriou V, Georgakopoulos E, Georgakopoulou S, Koliopanos A, Aggelakis F, Dardoufas K, Agnanti NJ, Karydas I, Nasioulas G. Cell-free DNA and RNA in plasma as a new molecular marker for prostate and breast cancer. Ann N Y Acad Sci 2006;1075:235-243.
12. Lin X, Tascilar M, Lee WH, Vles WJ, Lee BH, Veeraswamy R, Asgari K, Freije D, van Rees B, Gage WR, Bova GS, Isaacs WB, Brooks JD, DeWeese TL, De Marzo AM, Nelson WG. GSTP1 CpG island hypermethylation is responsible for the absence of GSTP1 expression in human prostate cancer cells. The American journal of pathology 2001;159(5):1815-1826.
13. Maruyama R, Toyooka S, Toyooka KO, Virmani AK, Zochbauer-Muller S, Farinas AJ, Minna JD, McConnell J, Frenkel EP, Gazdar AF. Aberrant promoter methylation profile of prostate cancers and its relationship to clinicopathological features. Clin Cancer Res 2002;8(2):514-519.
14. Yamanaka M, Watanabe M, Yamada Y, Takagi A, Murata T, Takahashi H, Suzuki H, Ito H, Tsukino H, Katoh T, Sugimura Y, Shiraishi T. Altered methylation of multiple genes in carcinogenesis of the prostate. International journal of cancer 2003;106(3):382-387.
15. Jeronimo C, Henrique R, Hoque MO, Mambo E, Ribeiro FR, Varzim G, Oliveira J, Teixeira MR, Lopes C, Sidransky D. A quantitative promoter methylation profile of prostate cancer. Clin Cancer Res 2004;10(24):8472-8478.

16. Kang GH, Lee S, Lee HJ, Hwang KS. Aberrant CpG island hypermethylation of multiple genes in prostate cancer and prostatic intraepithelial neoplasia. The Journal of pathology 2004;202(2):233-240.
17. Singal R, Ferdinand L, Reis IM, Schlesselman JJ. Methylation of multiple genes in prostate cancer and the relationship with clinicopathological features of disease. Oncology reports 2004;12(3):631-637.
18. Woodson K, Gillespie J, Hanson J, Emmert-Buck M, Phillips JM, Linehan WM, Tangrea JA. Heterogeneous gene methylation patterns among pre-invasive and cancerous lesions of the prostate: a histopathologic study of whole mount prostate specimens. Prostate 2004;60(1):25-31.
19. Yegnasubramanian S, Kowalski J, Gonzalgo ML, Zahurak M, Piantadosi S, Walsh PC, Bova GS, De Marzo AM, Isaacs WB, Nelson WG. Hypermethylation of CpG islands in primary and metastatic human prostate cancer. Cancer Res 2004;64(6):1975-1986.
20. De Marzo AM, Platz EA, Sutcliffe S, Xu J, Gronberg H, Drake CG, Nakai Y, Isaacs WB, Nelson WG. Inflammation in prostate carcinogenesis. Nature reviews 2007;7(4):256-269.
21. Peng DF, Razvi M, Chen H, Washington K, Roessner A, Schneider-Stock R, El-Rifai W. DNA hypermethylation regulates the expression of members of the Mu-class glutathione S-transferases and glutathione peroxidases in Barrett's adenocarcinoma. Gut 2009;58(1):5-15.
22. Bird A. DNA methylation patterns and epigenetic memory. Genes & development 2002;16(1):6-21.
23. Feinberg AP, Tycko B. The history of cancer epigenetics. Nature reviews 2004;4(2):143-153.
24. Esteller M. Epigenetics in cancer. The New England journal of medicine 2008;358(11):1148-1159.
25. Fang M, Chen D, Yang CS. Dietary polyphenols may affect DNA methylation. The Journal of nutrition 2007;137(1 Suppl):223S-228S.
26. Karpf AR, Jones DA. Reactivating the expression of methylation silenced genes in human cancer. Oncogene 2002;21(35):5496-5503.
27. Graff JR, Gabrielson E, Fujii H, Baylin SB, Herman JG. Methylation patterns of the E-cadherin 5' CpG island are unstable and reflect the dynamic, heterogeneous loss of E-cadherin expression during metastatic progression. J Biol Chem 2000;275(4):2727-2732.
28. Camoriano M, Kinney SR, Moser MT, Foster BA, Mohler JL, Trump DL, Karpf AR, Smiraglia DJ. Phenotype-specific CpG island methylation events in a murine model of prostate cancer. Cancer Res 2008;68(11):4173-4182.
29. McCabe MT, Low JA, Daignault S, Imperiale MJ, Wojno KJ, Day ML. Inhibition of DNA methyltransferase activity prevents tumorigenesis in a mouse model of prostate cancer. Cancer Res 2006;66(1):385-392.
30. Morey Kinney SR, Smiraglia DJ, James SR, Moser MT, Foster BA, Karpf AR. Stage-specific alterations of DNA methyltransferase expression, DNA hypermethylation, and DNA hypomethylation during prostate cancer progression in the transgenic adenocarcinoma of mouse prostate model. Mol Cancer Res 2008;6(8):1365-1374.
31. Morey SR, Smiraglia DJ, James SR, Yu J, Moser MT, Foster BA, Karpf AR. DNA methylation pathway alterations in an autochthonous murine model of prostate cancer. Cancer Res 2006;66(24):11659-11667.
32. Zorn CS, Wojno KJ, McCabe MT, Kuefer R, Gschwend JE, Day ML. 5-aza-2'-deoxycytidine delays androgen-independent disease and improves survival in the transgenic adenocarcinoma of the mouse prostate mouse model of prostate cancer. Clin Cancer Res 2007;13(7):2136-2143.
33. Greenburg NM, DeMayo F, Finegold MJ, Medina D, Tilley WD, Aspinall JO, Cunha GR, Donjacour AA, Matusik RJ, Rosen JM. Prostate cancer in a transgenic mouse. Proc Natl Acad Sci 1995:3439-3443.
34. Gingrich JR, Barrios RJ, Foster BA, Greenberg NM. Pathologic progression of autochthonous prostate cancer in the TRAMP model. Prostate Cancer Prostatic Dis 1999;2(2):70-75.

35. Gingrich JR, Barrios RJ, Kattan MW, Nahm HS, Finegold MJ, Greenberg NM. Androgen-independent prostate cancer progression in the TRAMP model. Cancer Res 1997;57(21):4687-4691.
36. Schmittgen TD ZB. Effect of experimental treatment on housekeeping gene expression: validation by real-time, quantitative RT-PCR. J Biochem Biophys Methods 2000;46:69-81.
37. Ehrich M, Nelson MR, Stanssens P, Zabeau M, Liloglou T, Xinarianos G, Cantor CR, Field JK, van den Boom D. Quantitative high-throughput analysis of DNA methylation patterns by base-specific cleavage and mass spectrometry. Proc Natl Acad Sci U S A 2005;102(44):15785-15790.
38. Foster BA, Gingrich JR, Kwon ED, Madias C, Greenberg NM. Characterization of prostatic epithelial cell lines derived from transgenic adenocarcinoma of the mouse prostate (TRAMP) model. Cancer Res 1997;57(16):3325-3330.
39. Frohlich DA, McCabe MT, Arnold RS, Day ML. The role of Nrf2 in increased reactive oxygen species and DNA damage in prostate tumorigenesis. Oncogene 2008;27(31):4353-4362.
40. Deeb KK, Michalowska AM, Yoon CY, Krummey SM, Hoenerhoff MJ, Kavanaugh C, Li MC, Demayo FJ, Linnoila I, Deng CX, Lee EY, Medina D, Shih JH, Green JE. Identification of an integrated SV40 T/t-antigen cancer signature in aggressive human breast, prostate, and lung carcinomas with poor prognosis. Cancer Res 2007;67(17):8065-8080.
41. Meiers I, Shanks JH, Bostwick DG. Glutathione S-transferase pi (GSTP1) hypermethylation in prostate cancer: review 2007. Pathology 2007;39(3):299-304.
42. Baylin SB, Herman JG, Graff JR, Vertino PM, Issa JP. Alterations in DNA methylation: a fundamental aspect of neoplasia. Advances in cancer research 1998;72:141-196.
43. Jones PA, Taylor SM. Cellular differentiation, cytidine analogs and DNA methylation. Cell 1980;20(1):85-93.
44. Yoshida M, Kijima M, Akita M, Beppu T. Potent and specific inhibition of mammalian histone deacetylase both in vivo and in vitro by trichostatin A. J Biol Chem 1990;265(28):17174-17179.
45. Cameron EE, Bachman KE, Myohanen S, Herman JG, Baylin SB. Synergy of demethylation and histone deacetylase inhibition in the re-expression of genes silenced in cancer. Nature genetics 1999;21(1):103-107.
46. Song F, Mahmood S, Ghosh S, Liang P, Smiraglia DJ, Nagase H, Held WA. Tissue specific differentially methylated regions (TDMR): Changes in DNA methylation during development. Genomics 2009;93(2):130-139.
47. Song F, Smith JF, Kimura MT, Morrow AD, Matsuyama T, Nagase H, Held WA. Association of tissue-specific differentially methylated regions (TDMs) with differential gene expression. Proc Natl Acad Sci U S A 2005;102(9):3336-3341.
48. Suzuki M, Sato S, Arai Y, Shinohara T, Tanaka S, Greally JM, Hattori N, Shiota K. A new class of tissue-specifically methylated regions involving entire CpG islands in the mouse. Genes Cells 2007;12(12):1305-1314.
49. Tam NN, Nyska A, Maronpot RR, Kissling G, Lomnitski L, Suttie A, Bakshi S, Bergman M, Grossman S, Ho SM. Differential attenuation of oxidative/nitrosative injuries in early prostatic neoplastic lesions in TRAMP mice by dietary antioxidants. The Prostate 2006;66(1):57-69.

FIGURE LEGENDS

Fig. 1. *Gst* mRNA expression in normal prostates from WT mice and TRAMP tumors. qRT-PCR of *Gst* genes was performed as described in *Materials and Methods* using the samples described in Table 1. *Gst* mRNA copy number is plotted relative to 18s rRNA expression. (**A**) *Gst* expression in normal murine prostate (N = 15). *Gst* family members analyzed are shown on the x-axis. (**B**) *GstA4* (**C**) *GstK1* (**D**) *GstM1* (**E**) *GstO1* and (**F**) *GstP1* mRNA expression in normal prostate (N), primary prostate tumor (P), and metastases (M) (N = 15/group). The metastases group includes lymph node, kidney, and liver metastases (5 each). Error bars = Standard deviation (SD). The results of unpaired two-tailed T-test comparisons are shown for the indicated groups. In all cases, differences in *Gst* mRNA expression between Normal Prostate and Metastatic tumors were not significant.

Fig. 2. Western blot analysis of GstM1 and GstP1 protein expression in normal prostates from WT mice and TRAMP tumors. Cytosolic GstM1 and GstP1 protein levels were measured as described in *Materials and Methods* using the samples described in Table 1. (**A**) GstM1 Western blots. (**B**) GstP1 Western blots. Data labels: Normal prostates (N), primary tumors (P), kidney metastases (KM), liver metastases (LM), and lymph node metastases (LNM). For both panels, Ponceau S total protein staining served as a loading control.

Fig. 3. 5' end of murine Gst genes, indicating position of CpG islands and primer sites used for DNA methylation analyses. (**A**) *GstA4*, (**B**) *GstK1*, (**C**) *GstM1*, (**D**) *GstO1*, and (**E**) *GstP1*. For each diagram, the predicted transcriptional start sites from the UC Santa Cruz Genome Browser are shown with bent right arrows, and exons are shown with black filled bars. Hash marks indicate CpG sites. Gray filled bars show 5' CpG islands; CpG island characteristics as determined using CpG island searcher (http://www.uscnorris.com/cpgislands2/cpg.aspx) are shown beneath the gray bars. The approximate

position and 5' nucleotide coordinates of primers used for MAQMA methylation analysis are shown by inward facing arrows.

Fig. 4. Gst gene methylation in normal murine prostate and inverse association with *Gst* mRNA expression. (**A**) DNA methylation of the 5' regions of Gst genes diagrammed in Fig. 4 were determined by MassARRAY Quantitative DNA Methylation Analyses (MAQMA) as described in the *Materials and Methods*. Results plotted are the average methylation value of all CpG sites over the entire sequenced region, and all data are averaged over 5 normal prostate samples. Error bars = SD. (**B**) Gst methylation values plotted against *Gst* mRNA expression values shown in Fig. 1A. Non-linear regression (one-phase decay) correlation coefficient R^2 value was caculated using GraphPad Prism and is shown. (**C**) Gst methylation values plotted against *Gst* mRNA expression values shown in Fig. 1A, after removal of GstA4 data. Correlation coefficient R^2 value was calculated as described in panel C. Symbols : square = GstM1; circle = GstA4; inverted triangle = GstP1; diamond = GstO1; triangle = GstK1.

Fig. 5. Individual CpG site DNA methylation of Gst genes in normal prostates from WT mice and TRAMP tumors. (**A**) *GstA4*, (**B**) *GstK1*, (**C**) *GstM1*, (**D**) *GstO1*, and (**E**) *GstP1*. DNA methylation of the 5' regions of Gst genes diagrammed in Fig. 3 were determined by MassARRAY Quantitative DNA Methylation Analyses (MAQMA) as described in the *Materials and Methods*. Results plotted are the average methylation value of each CpG site (or clusters of CpG sites) within each sequenced region, and data are averaged for normal prostate (N) (N=5), primary tumor (P) (N=15), and metastatic tumors (M) (N = 15). Infrequently, CpG sites failed MAQMA analysis; in these instances no data are shown (absence of bars on the graph). Right arrows below X-axes indicate the approximate position of the predicted transcriptional start site for each gene. Error bars = SD.

Fig. 6. Averaged Gst gene methylation in normal prostates from WT mice and TRAMP tumors. (**A**) *GstA4*, (**B**) *GstK1*, (**C**) *GstM1*, (**D**) *GstO1*, and (**E**) *GstP1*. DNA methylation of the 5' regions of Gst genes diagrammed in Fig. 3 were determined by MassARRAY Quantitative DNA Methylation Analyses (MAQMA) as described in the *Materials and Methods*. Results plotted are the average methylation value of all CpG sites over the entire sequenced region, and all data are averaged for normal prostates (N) (N=5), primary tumors (P) (N=15), and metastatic tumors (M) (N = 15). The methylation data for the individual sites comprising each region are shown in Fig. 5. Error bars = SD. In all cases, the differences between groups were not significant (data not shown).

Fig. 7. Effect of decitabine and TSA treatment on Gst gene expression in TRAMP-C2 cells. TRAMP-C2 cells were treated with 1.0 μM decitabine (DAC) and/or 600 nM trichostatin A (TSA) as described in the *Materials and Methods*, and cells were harvest at five days post-DAC treatment and/or one day post TSA treatment. The vehicle control consisted of treatment of TRAMP-C2 cells with PBS and DMSO for five days and one day, respectively. Gst mRNA expression was measured by qRT-PCR as described in the *Materials and Methods*. (**A**) *GstA4*, (**B**) *GstK1*, (**C**) *GstM1*, (**D**) *GstO1*, and (**E**) *GstP1*. Error bars = SD. Students T-test (unpaired, one-tailed) was performed to test for significant differences in Gst gene expression between control cells and cells treated with DAC and TSA. Results (P-values) are shown on the figure.

Supplemental Fig. 1. Representative Immunohistochemical (IHC) staining of (**A**) GstM1 and (**B**) GstP1 in normal ventral prostate from WT mice and primary TRAMP tumors arising in the ventral prostate lobe. IgG control staining of normal prostate, and Gst antibody staining of normal prostate and TRAMP primary tumors is shown. All images shown are 10X magnification.

Table 1. Samples used.

Tissue Type	Mouse Strain	# of Samples	Age (weeks ± SD)	Urogenital Tract Weight (mgs ± SD)	Prostate Weight (mgs ± SD)
Normal	50:50 C57Bl/6:FVB Wildtype (WT)	15	22.9 ± 8.0	0.57 ± 0.2	0.02 ± 0.00
Primary Tumor	" " TRAMP	15	25.9 ± 4.5	6.21 ± 2.5	5.67 ± 3.8
Kidney Metastasis	" " TRAMP	5	26.8 ± 6.9	6.51 ± 10.7	9.12 ± 13.8
Liver Metastasis	" " TRAMP	5	26.4 ± 8.3	3.97 ± 4.2	2.00 ± 4.2
Lymph Node Metastasis	" " TRAMP	5	31.8 ± 6.5	7.95 ± 6.2	7.93 ± 7.0

Fig. 1. Mavis et al.

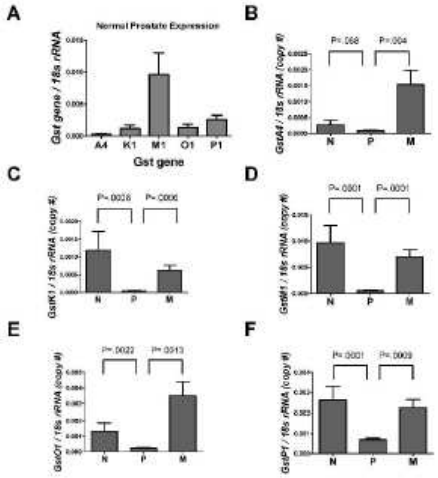

279x215mm (600 x 600 DPI)

Fig. 2. Mavis et al.

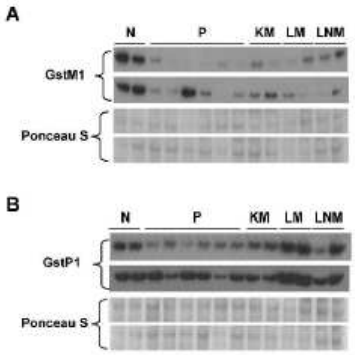

279x215mm (600 x 600 DPI)

Fig 3.

Mavis et al.

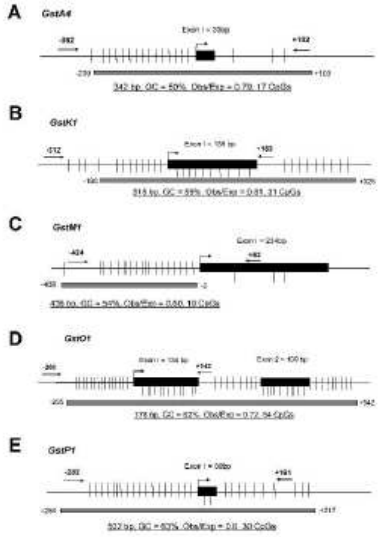

279x215mm (600 x 600 DPI)

Fig 4.

Mavis et al.

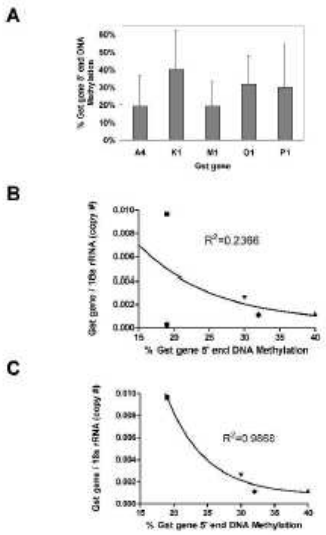

279x215mm (600 x 600 DPI)

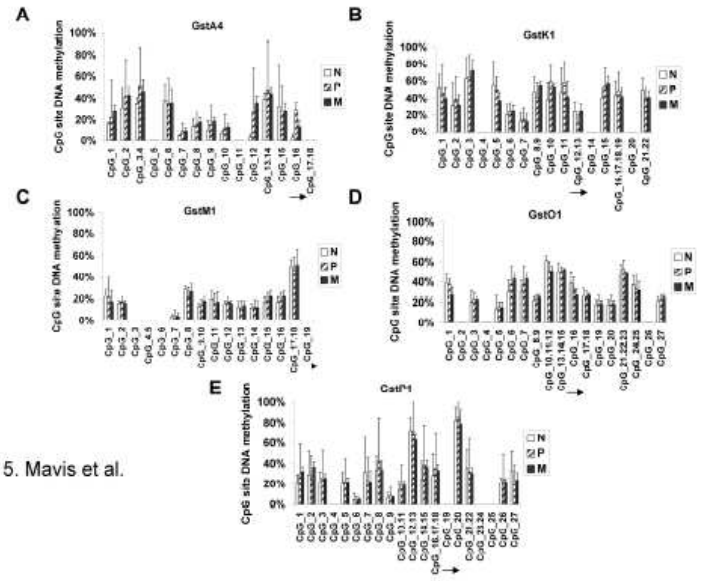

Fig 5. Mavis et al.

279x215mm (600 x 600 DPI)

Fig 6. Mavis et al.

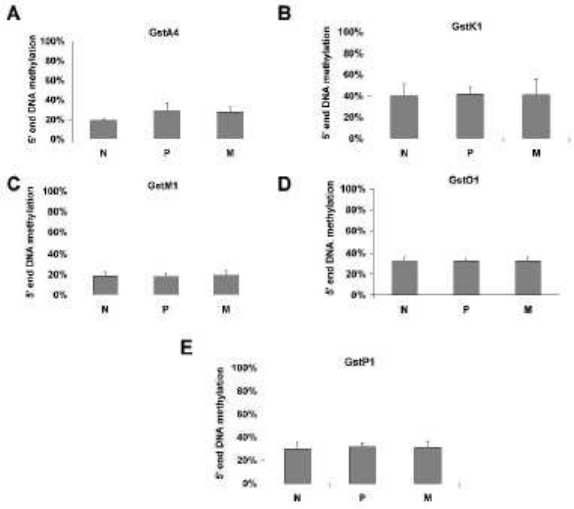

279x215mm (600 x 600 DPI)

Fig 7. Mavis et al.

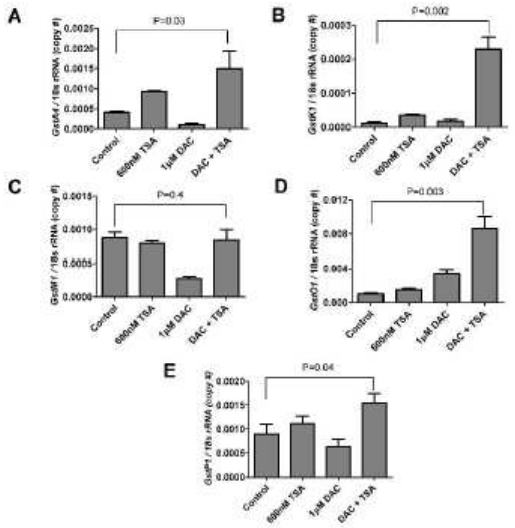

279x215mm (600 x 600 DPI)

Supplemental Table 1. Primer Sequences.

Gene	Assay	Sequence	5' position relative to TSS [1]	Annealing Temperature
GstA4	qRT-PCR[2]	F: 5' - TCCCACAAGAATAAGGAAGCTC - 3'	(+) 37	62ºC
	qRT-PCR	R: 5' - GGTGTCCATCCTTTTGCATC - 3'	(+) 219	62ºC
	MAQMA[3]	F: 5' - TTGTTGGTAATGAATATAATGAATTTATAA - 3'	(-) 352	68°C
	MAQMA	R: 5' - ACAAAAAAAATACACACACACACAC - 3'	(+) 102	68°C
GstK1	qRT-PCR	F: 5' - CATGAAAGACAGCGGAAACC - 3'	(+) 226	60ºC
	qRT-PCR	R: 5' - ATACTTCCTTTCTTCACAGTCT - 3'	(+) 375	60ºC
	MAQMA	F: 5' - TTGTTTTTATTTTTGAGAAAGTGAATATAA - 3'	(-) 312	65.8°C
	MAQMA	R: 5' - CACCTCAAAACCCAACCAAAAATAC -3'	(+) 162	65.8°C
GstM1	qRT-PCR	F:5' - CCTGGATGGAGAGACAGAGG - 3'	(+) 454	60ºC
	qRT-PCR	R: 5' - GACCTTGTCCCCTGCAAA - 3'	(+) 658	60ºC
	MAQMA	F: 5' - TTGTTTTTGTAATTTGAGGTTGTGTG - 3'	(-) 424	70.9°C
	MAQMA	R: 5' - CAATTAAACACTCCCCTTCCTAAATCTATA - 3'	(+) 62	70.9°C
GstO1	qRT-PCR	F: 5' - CTAAGGTGCCGCCTTTGA - 3'	(+) 462	60ºC
	qRT-PCR	R: 5' - CTCCTTGAGCTCCAATGCTT - 3'	(+) 670	60ºC
	MAQMA	F: 5' - GGGATGGGGTGGTTTTTTTTGAGTATT - 3'	(-) 260	71.3°C
	MAQMA	R: 5' - AACCTCACCCTTCCCCAAACTCCTA - 3'	(+) 142	71.3°C
GstP1	qRT-PCR	F: 5' - AGCAGGCATGCCACCATA - 3'	(+) 43	60ºC
	qRT-PCR	R: 5' - GCTGCCCATACAGACAAGTG - 3'	(+) 206	60ºC
	MAQMA	F: 5' - GGGATAGGTAAAAGGTTGATAGAGTTGTAT - 3'	(-) 282	73.2ºC
	MAQMA	R: 5' - CCCAAACTCCTATTACAAACTACCC - 3'	(+) 161	73.2ºC

[1] Transcriptional Start Site as determined using the UC Santa Cruz genome browser (http://genome.ucsc.edu/)

[2] Quantitative real time reverse transcriptase PCR

[3] MassARRAY Quantitative DNA Methylation Analyses

Supplemental Fig. 1. Mavis et al.

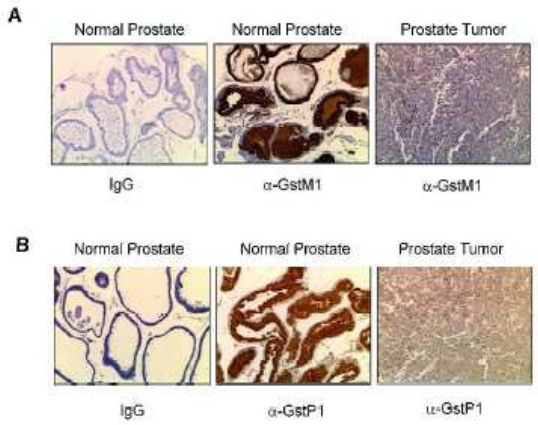

279x215mm (600 x 600 DPI)